

Transcriptomic response of sea urchin larvae *Strongylocentrotus purpuratus* to CO₂-driven seawater acidification

Anne E. Todgham* and Gretchen E. Hofmann[†]

Department of Ecology, Evolution, and Marine Biology, University of California Santa Barbara, Santa Barbara, CA 93106, USA

*Present Address: Department of Biology, San Francisco State University, San Francisco, CA 94132, USA

[†]Author for correspondence (e-mail: hofmann@lifesci.ucsb.edu)

Accepted 18 May 2009

SUMMARY

Ocean acidification from the uptake of anthropogenic CO₂ is expected to have deleterious consequences for many calcifying marine animals. Forecasting the vulnerability of these marine organisms to climate change is linked to an understanding of whether species possess the physiological capacity to compensate for the potentially adverse effects of ocean acidification. We carried out a microarray-based transcriptomic analysis of the physiological response of larvae of a calcifying marine invertebrate, the purple sea urchin, *Strongylocentrotus purpuratus*, to CO₂-driven seawater acidification. In lab-based cultures, larvae were raised under conditions approximating current ocean pH conditions (pH8.01) and at projected, more acidic pH conditions (pH7.96 and 7.88) in seawater aerated with CO₂ gas. Targeting expression of ~1000 genes involved in several biological processes, this study captured changes in gene expression patterns that characterize the transcriptomic response to CO₂-driven seawater acidification of developing sea urchin larvae. In response to both elevated CO₂ scenarios, larvae underwent broad scale decreases in gene expression in four major cellular processes: biomineralization, cellular stress response, metabolism and apoptosis. This study underscores that physiological processes beyond calcification are impacted greatly, suggesting that overall physiological capacity and not just a singular focus on biomineralization processes is essential for forecasting the impact of future CO₂ conditions on marine organisms. Conducted on targeted and vulnerable species, genomics-based studies, such as the one highlighted here, have the potential to identify potential 'weak links' in physiological function that may ultimately determine an organism's capacity to tolerate future ocean conditions.

Key words: early development, global change, microarray, ocean acidification, sea urchin, transcriptomics.

INTRODUCTION

Ocean acidification (OA) has been recently recognized as one of the most pervasive and potentially damaging anthropogenic impacts on life in oceans (Halpern et al., 2008). Acting as a sink for atmospheric carbon dioxide (CO₂), within the last 200 years the oceans have absorbed approximately 50% of anthropogenic CO₂ emissions (Sabine et al., 2004). Elevated atmospheric CO₂ dissolves into seawater driving a chemical equilibrium such that the pH of the ocean becomes less alkaline. Awareness of the potentially deleterious effects of OA, perhaps raised most notably by Kleypas et al. in 1999 (Kleypas et al., 1999), was a driver for research that has now demonstrated significant impacts on important marine calcifiers, largely because of the sensitivity of calcification rates to elevated CO₂ [summarized by Fabry et al. (Fabry et al., 2008) and Doney et al. (Doney et al., 2009)]. Given the measured impacts of low pH seawater on organismal function (Seibel and Walsh, 2003; Pörtner et al., 2005), and the dominance of calcifying organisms in many, if not most, marine ecosystems, the vulnerability of entire marine communities in the face of OA is apparent. Ecosystems ranging from polar oceans to tropical coral reefs are threatened (Guinotte and Fabry, 2008). In fact, very recent studies in the field have provided some of the first potential direct links between OA and shifting marine communities, illustrating how organismal physiology, driven by changes in ocean partial pressure of CO₂ (P_{CO_2}), will influence the structure of future marine ecosystems (Manno et al., 2007; Cooper et al., 2008; Hall-Spencer et al., 2008; Wootton et al., 2008; De'ath et al., 2009).

Increasingly, it is apparent that physiologists have an important role in understanding the ecological consequences of global climate change (e.g. Pörtner, 2008; Pörtner and Farrell, 2008; Widdicombe and Spicer, 2008). Of critical importance to our understanding of the vulnerability of organisms to OA is whether particular species currently possess the physiological capacity to compensate or adjust for the potentially deleterious impacts of OA, what the costs of this compensation might be, and furthermore, whether populations have sufficient genetic variation and time to adapt to these unprecedented rates of climate change (e.g. Hoegh-Guldberg et al., 2007; Bell and Collins, 2008). An important first step is being able to identify key physiological mechanisms that may underlie an organism's ability or inability to cope with the unprecedented rate of change in ocean chemistry. From an organismal perspective, an accumulating body of research suggests that many taxonomic groups stand to be impacted with effects ranging from changes in calcification (Riebesell et al., 2000; Langdon and Atkinson, 2005; Gazeau et al., 2007; Kurihara et al., 2007; Iglesias-Rodriguez et al., 2008; Kuffner et al., 2007), growth (Harris et al., 1999; Michaelidis et al., 2005; Shirayama and Thornton, 2005; Berge et al., 2006; Hauton et al., 2009), metabolism (Reipschläger and Pörtner, 1996; Pörtner et al., 1998; Michaelidis et al., 2005; Rosa and Seibel, 2008), reproduction and development (Kurihara and Shirayama, 2004; Kurihara et al., 2007; Mayor et al., 2007; Dupont et al., 2008), survival (Watanabe et al., 2006; Dupont et al., 2008) and photosynthesis (Fu et al., 2007). These initial, descriptive studies provide us with important insight into the potential impacts of elevated CO₂ on the function of marine organisms.

Research addressing the physiological mechanisms underlying long-term or chronic sensitivity to the altered ocean chemistry that characterizes OA is less numerous. There is, however, substantial literature from comparative physiologists on the acute effects of hypercapnia, or high P_{CO_2} , on marine organisms (Cameron, 1986; Truchot, 1987; Heisler, 1989; Pörtner, 2008). Although these hypercapnic exposures are very high compared to the levels predicted for OA (e.g. 10,000 p.p.m. CO_2 , more relevant to carbon sequestration, as compared with 1000 p.p.m. CO_2 , a likely emission scenario predicted by the Intergovernmental Panel on Climate Change for 2100), these studies have provided information on the mechanisms underlying acid–base regulation and the other closely coordinated physiological processes such as ion regulation, metabolism and protein synthesis (for a review, see Pörtner et al., 2005). These studies have highlighted that calcifying as well as non-calcifying, organisms show many similar responses to elevated CO_2 , suggesting that the unifying physiological mechanisms underlying sensitivity to OA are more a direct result of the low pH and increased P_{CO_2} than the decreased availability of carbonate ion in the oceans. Although there is no doubt that elevated CO_2 has dramatic impacts on calcification, it is known that the transport of carbon across epithelia to sites of calcification in a diversity of taxa is generally in the form of bicarbonate (HCO_3^-) and not carbonate (CO_3^{2-}) (e.g. McConnaughey and Whelan, 1997; Cohen and McConnaughey, 2003; Wilt, 2005). Taken together these findings provide strong evidence that research needs to expand its focus beyond calcification to investigate additional physiological processes if we are to understand the mechanisms underlying sensitivity of marine organisms to OA.

In the post-genomic era, we have access to a number of sensitive genomics-enabled techniques to investigate simultaneously the molecular response of many cellular pathways to a common stressor. Although there are a diversity of mechanisms for regulating cellular pathways (e.g. through allosteric modulation or mass action) gene regulation is one of the most rapid and versatile ways in which an organism can respond to an environmental stressor. Since the ability of an organism to adjust to a changing environment will be driven by complex changes in gene regulatory networks and subtle changes in numerous cellular pathways, the use of genomics tools will be particularly useful in elucidating the early responses to OA. Suites of differentially regulated genes can provide a physiological signature of organismal condition as well as uncover the molecular mechanisms conferring physiological plasticity (Gracey, 2007). DNA microarrays provides us with a great deal of information on the variance in the transcriptome, or the suite of mRNA transcripts expressed in the cell at a given time. The use of array-based transcriptomics has been a very fruitful avenue of research to understand the molecular responses to a variety of environmental stressors in the lab, such as temperature change (Gracey et al., 2004; Buckley et al., 2006; Teranishi and Stillman, 2007; DeSalvo et al., 2008), osmotic stress (Evans and Somero, 2008), and hypoxia (Gracey et al., 2001; Olohan et al., 2008). More recently this transcriptomics approach has been implemented successfully in field studies providing us with gene expression profiles of organisms undergoing natural changes in their environment and subsequently insight into what aspects of environmental change the animal is responding to (e.g. Gracey et al., 2008; Place et al., 2008). Gene expression studies are an excellent approach for understanding the broad and integrated responses to OA that are initiated at the level of the transcriptome. In turn, these types of data can inform us about physiological thresholds of present day populations and their potential to tolerate future climate change scenarios.

In this study, we have used gene expression profiling in a marine calcifier, larvae of the purple sea urchin, *Strongylocentrotus purpuratus*, a key benthic invertebrate in coastal temperate ecosystems of North America (Pearse, 2006), to begin to explore the physiological mechanisms that may underlie tolerance to future OA conditions. These larvae are ideal for this study because larval echinoderms are well known to show distinct plasticity in their developmental trajectories (Hart and Strathmann, 1994), their calcite skeletons and body form in general are altered under low pH and low carbonate conditions (Kurihara, 2008; DuPont et al., 2008; O'Donnell et al., 2009b) and the genome of the purple sea urchin has been sequenced and largely annotated (Sea Urchin Genome Sequencing Consortium, 2006) Using atmospheric CO_2 emission scenarios predicted for the year 2100 by the Intergovernmental Panel on Climate Change (IPCC) as an experimental framework (Intergovernmental Panel on Climate Change, 2007), we raised urchin larvae under different atmospheric CO_2 conditions and used a DNA oligonucleotide microarray to profile gene expression in early prism larvae, an early development stage that is entering a rapid stage of growth and actively synthesizing a CaCO_3 endoskeleton. This study provides a high-resolution method of examining the sub-lethal effects of CO_2 -driven seawater acidification at the molecular level and allows us to begin to identify the cellular pathways that are involved in the purple urchin's capacity to respond to future climate change.

MATERIALS AND METHODS

Urchin collection and spawning

Adult *Strongylocentrotus purpuratus* Stimpson 1857 were collected by SCUBA divers around Goleta Pier (Goleta, CA, USA) and maintained in flowing seawater tables at 15–16°C in the Marine Science Institute at the University of California Santa Barbara for 2 days prior to spawning. Spawning was induced by coelomic injection of 0.5 mol l⁻¹ KCl following standard methods (Strathmann, 1987). Eggs were collected from three females and separately fertilized by sperm from a single male. This resulted in three replicate urchin cultures in which larvae within a culture were full-siblings and larvae between cultures were half-siblings. Only batches of eggs with a fertilization rate of at least 95% were used for experimentation to ensure selection of good quality embryos.

CO_2 incubations of larval sea urchin cultures

Larval *S. purpuratus* were cultured in seawater bubbled with three different concentrations of CO_2 , which were chosen to reflect the CO_2 emission scenarios predicted by the Intergovernmental Panel on Climate Change (Intergovernmental Panel on Climate Change, 2007) for the year 2100. Culture chambers were aerated continuously with commercially manufactured air premixed at these three different concentrations: 380 p.p.m. CO_2 (present day atmospheric CO_2 level), ~540 p.p.m. CO_2 , an optimistic atmospheric CO_2 concentration predicted by the IPCC (B1 scenario) and ~1020 p.p.m. CO_2 , a more 'business as usual' emission scenario (A1FI). The above CO_2 aeration regimes resulted in seawater in which our three larval treatment groups were raised, having the following pHs: pH 8.01±0.01 for the 380 p.p.m. CO_2 condition (Control CO_2), pH 7.96±0.01 for the 540 p.p.m. CO_2 condition (Moderate CO_2), and pH 7.88±0.02 for the 1020 p.p.m. CO_2 condition (High CO_2).

Larvae were cultured in a 15 l nested bucket culture chamber design. The internal bucket was drilled with twelve 3 inch (7.5 cm)-diameter holes and was isolated from the outer bucket by covering these holes with 64 µm mesh. Each bucket pair was fitted with an external PVC side arm connecting the bottom space of the outer

bucket (5l), which contained no larvae, to the internal bucket (10l) with a short diffusing pipe along one side. The side-arm provided a location to aerate the culture water with gas away from the developing larvae and in turn generated a slow mixing current for the larvae within the inside bucket. Gas was bubbled to each culture chamber at a rate of 75 ml min^{-1} . The culture chambers were filled with seawater that was replaced at a rate of 0.5 l h^{-1} to provide fresh seawater without altering the pH. Experiments were not started, and therefore the urchins were not spawned, until the pH of each culture chamber had stabilized for at least 24h. Water temperature was $15 \pm 0.5^\circ\text{C}$ and dissolved oxygen levels did not fall below $7.9 \text{ mg O}_2 \text{ l}^{-1}$. The pH of each chamber was monitored daily using a Radiometer Analytical PHM240 pH meter.

Following fertilization, each of the three replicate sea urchin larval cultures was divided in three such that there were three replicate cultures for each of the three CO_2 treatment conditions (i.e. a total of nine cultures). Fertilization of each batch of eggs was staggered by 2h to allow us to closely monitor developmental timing and sample larvae based on their stage and not based on their time post-fertilization. Larval development in each of the nine cultures was assessed at mid-gastrula ($\sim 29 \text{ h}$ post-fertilization), an early prism ($\sim 40 \text{ h}$ post-fertilization) and an early echinopluteus stage ($\sim 70 \text{ h}$ post-fertilization). The timing of development varied slightly (within

1 h) between cultures from the three different females, but there were no visible differences in developmental timing as an effect of CO_2 treatment during the course of this experiment (see Fig. 1). In addition, there were no obvious developmental abnormalities for any of the stages and no mortality associated with any of the CO_2 treatments. Larvae were not fed during the experiments because of the short duration of the experiment ($< 72 \text{ h}$).

When larvae had reached an early prism stage ($\sim 40 \text{ h}$ post-fertilization), a sample of larvae was removed from each of the nine culture chambers for later gene expression analysis, using a custom-designed oligonucleotide microarray and quantitative PCR. Larvae from each sample were quickly pelleted by centrifugation for 5s, the seawater was removed and 1 ml of TRIzol[®] Reagent (Invitrogen, Carlsbad, CA, USA) was added. In order to rupture the larvae, samples were quickly vortexed, then passed slowly through a 21 gauge needle followed by a 25 gauge needle (three passes for each needle size) and frozen at -80°C for later RNA extraction.

RNA extraction

Total RNA was extracted from a sample of approximately 60,000 larvae from each of the three replicate cultures at each of the three CO_2 culture treatments (nine samples in total). Total RNA was isolated using the guanidine isothiocyanate method outlined by

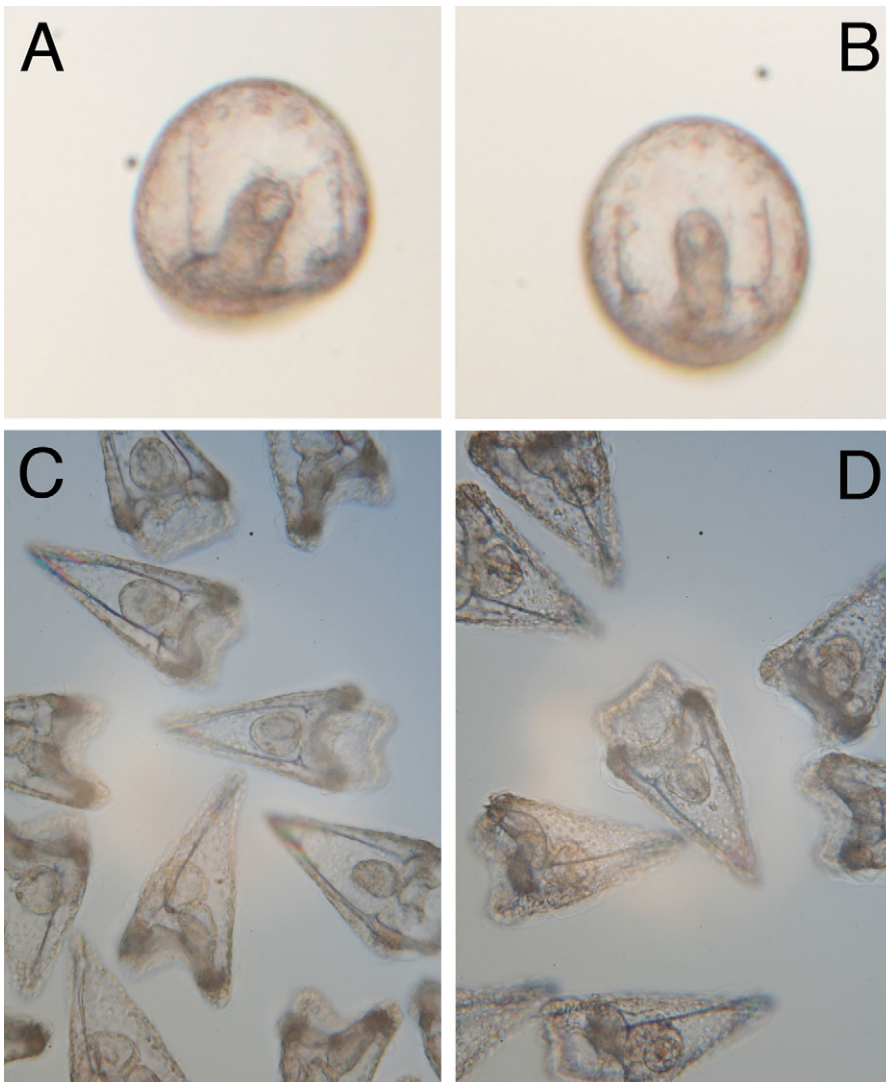


Fig. 1. *Strongylocentrotus purpuratus*. Representative early prism (40 h post-fertilization; A,B) and early echinopluteus larvae (70 h post-fertilization; C,D) from replicate culture #1 following development under Control CO_2 (A,C) or High CO_2 treatments (B,D).

Chomczynski and Sacchi (Chomczynski and Sacchi, 1987) using TRIzol[®] Reagent. Following extraction, RNA was processed through an additional clean-up step to remove tRNA and small-sized RNA degradation products. Dried total RNA pellets were resuspended in 0.1 ml of nuclease-free water. Following resuspension, 0.3 ml of 6 mol l⁻¹ guanidine hydrochloride and 0.2 ml of 100% ethanol were added and the entire volume was loaded onto a filter cartridge (Applied Biosystems, Foster City, CA, USA and Ambion, Austin, TX, USA) and centrifuged for 1 min at 12,000 g at room temperature. Flow-through was discarded and filters were washed twice with 0.2 ml of 80% ethanol. RNA was eluted off the filters twice with 0.1 ml nuclease-free water. To precipitate RNA, 0.1 vol of 3 mol l⁻¹ sodium acetate (pH 5.0) and 2.5 vol of 100% ethanol was added to the eluted RNA, the contents were mixed by vortexing and then incubated for 1 h at -80°C. After this period, tubes were centrifuged at 12,000 g for 20 min at 4°C. Pellets were rinsed twice with 80% ethanol and resuspended in 30 µl of nuclease-free water. RNA was quantified spectrophotometrically using a ND-1000 UV/visible spectrophotometer (NanoDrop Technologies, Wilmington, DE, USA) and electrophoresed on a 1.5% w/v agarose gel to verify RNA integrity. RNA was stored at -80°C.

Gene expression profiling with oligonucleotide microarrays

Microarray analysis was performed using a custom-designed oligonucleotide microarray developed to screen the expression patterns of genes central to the calcification process, acid-base compensation and ion regulation, the cellular stress response, apoptosis, cell cycle, development, metabolism, translational control of proteins and cell signaling in purple sea urchins (Sea Urchin Genome Sequencing Consortium, 2006). Gene sequences were obtained from the Sea Urchin Genome Project public database (Baylor College of Medicine, <http://annotation.hgsc.bcm.tmc.edu/Urchin/cgi-bin/pubLogin.cgi>). Each of the 1057 genes on the microarray was represented by up to three different 60 base pair oligonucleotide probes generated using YODA (Yet-another Oligonucleotide Design Application) (Nordberg, 2005) and printed in triplicate on the microarray. This 8958-feature microarray was then multiplexed and printed four separate times on each slide (manufactured by Agilent Technologies, Santa Clara, CA, USA).

Microarray analysis was performed on larvae that were raised under the three different CO₂ conditions to an early prism stage (~40 h post-fertilization). First strand cDNA was synthesized from 10 µg of total RNA using anchored oligo(dT₂₃V) and pdN6 random hexamer primers, amino-allyl dUTP and SuperScript III reverse transcriptase (Invitrogen). Each sample was labeled by indirect coupling with either Alexa Fluor 555 or Alexa Fluor 647 succinimidyl ester dyes (Invitrogen). The cDNA samples were checked spectrophotometrically (Nanodrop Technologies) to ensure high quality cDNA synthesis (>600 ηg) and dye incorporation (>8.0 pmol dye per µg cDNA) before continuing to slide hybridization. The larval cDNA sample from each replicate Moderate CO₂ or High CO₂ culture was competitively hybridized against the Control CO₂ culture from the same-replicate female. Using dye swaps of technical replicates, treatment effects could be estimated independently of dye effects. This microarray design resulted in six arrays for each of the Control CO₂ versus Moderate CO₂ and the Control CO₂ versus High CO₂ comparisons.

Microarray normalization and statistical analysis

Data from the 12 microarrays were extracted using GenePix Pro 4.0 software (Molecular Devices, Sunnyvale, CA, USA). The data discussed here have been deposited in the National Center for

Biotechnology Information (NCBI) Gene Expression Omnibus (GEO; www.ncbi.nlm.nih.gov/geo/) and are accessible through the GEO series accession number GSE13777. Normalization and data analysis were completed using R (R Development Core Team, 2008) with the limma software package (Linear Models for Microarray Data) (Smyth, 2005). Intensity-dependent lowess normalization is the most commonly used method for eliminating labeling bias in dual channel microarray platforms (Yang et al., 2002). The targeted array used in this experiment was designed to be a 'stressor'-responsive chip with 50% of the genes attributed to the defenseome, biomineralization pathways, acid-base balance and ion regulation and apoptosis. To avoid violating assumptions of the number or degree of symmetry of differentially expressed genes, a global normalization for dye-bias was applied on a probe-by-probe basis, after averaging over log ratios from replicate probes within arrays, by including a dye effect in the linear model. Analysis of differential expression was based on empirical Bayes-moderated *t*-statistics (Smyth, 2004) and completed using R. A list was generated of the mean log fold change (FC) of gene expression and the corresponding moderated standard deviation (s.d.) of the genes that demonstrated statistically significant (*P*<0.05) expression differences between the Control and Moderate CO₂ treatments and between the Control and High CO₂ treatments. These moderated standard deviations were then used to back transform the log FCs to the upper (FCUL) and lower (FCLL) limits of fold changes in expression.

Gene expression profiling with quantitative PCR

Results from the microarray analysis were validated by measuring mRNA expression of a number of biomineralization and energy metabolism genes in the same larval RNA samples from the Control CO₂ and Moderate CO₂ groups using quantitative real-time PCR (qPCR). The relative levels of mRNA for *cyclophilin 1* (SPU_007484), *MSP130* (SPU_013821), *COLP3α* (SPU_003768), *P16* (SPU_018408), *Suclg1* (SPU_025397), *Idh3a* (SPU_027710), *Sdhb* (SPU_026295), *Atp5d* (SPU_028873), *Cox5b* (SPU_019685), *Ndufs6* (SPU_019206), and *β-actin* (NM_214469) in early prism larvae were determined using qPCR on an iCycler Thermal Cycler (Bio-Rad). Gene-specific primers were designed using Primer Express software (version 2.0.0; Applied Biosystems, Foster City, CA, USA). Primer sequences are listed in Table 1. Quantitative PCR reactions were performed with 2 µl cDNA, 5 pmoles of each primer and 2× SYBR Green Master Mix (Bio-Rad) to a total volume of 22 µl. All qPCR reactions were run as follows: 1 cycle of 94°C for 3 min, 40 cycles of 94°C for 20 s, 55°C for 20 s, 1 cycle of 94°C for 1 min, 1 cycle of 55°C for 1 min. At the end of each PCR reaction, PCR products were subjected to a melt curve analysis to confirm the presence of a single amplicon.

To quantify *cyclophilin 1*, *MSP130*, *COLP3α*, *P16*, *Suclg1*, *Idh3a*, *Sdhb*, *Atp5d*, *Cox5b*, *Ndufs6* mRNA expression, one control cDNA sample was used to develop a standard curve for all primer sets relating threshold cycle to cDNA amount and this standard curve was run on each plate. All results were expressed relative to these standard curves and mRNA values were normalized relative to that of *β-actin* (see Table 1 for primer information). *β-actin* is a commonly used control gene in qPCR and specifically *β-actin* mRNA expression did not change in response to elevated CO₂ levels (data not shown), making it an appropriate internal control gene for this study.

RESULTS AND DISCUSSION

Recent global climate change models predict that ocean surface pH will fall by an estimated 0.2 to 0.4 units over the next century

Table 1. Sequences for gene-specific primers used in quantitative PCR

Gene	Forward primer (5' → 3')	Reverse primer (5' → 3')
<i>cyclophilin</i>	CTTCATGATCCAAGGTGGTGACT	CCATAGATGCTCCTGCTTCCA
<i>MSP130</i>	CCGAGGTCCAGCGATTGA	CACCCAACCTGACCTGTGTAAGG
<i>COLP3α</i>	TTCCGCTCCTCGCCTTT	GTGGCGTAATAGTTGCATTTGC
<i>P16</i>	AGATGGAACCTCTGGCAGTCA	CGGAGGGACCCATGTCAAC
<i>Suclg1</i>	CAAGGTTATCTGCCAGGGAATC	CAATGGCTTGGGTTGTATGGA
<i>Idh3a</i>	CCTCTGTGCAGCAAATTTTCAG	GTTACATCCACAGCCTCCATT
<i>Sdhb</i>	TGAACATCAACGGCACCAATA	TGCTTGAACCCCGGTCAATA
<i>Atp5d</i>	TGAGCAGTGGTATGATCACAGTCA	GCTGCCATCTCTGCAAGAATC
<i>Cox5b</i>	TACAGTCAAAGTTCAAGAGCAATGG	TGTGGCATGTTCAAAGTTGTCA
<i>Ndufs6</i>	TCCATGAAGAACCACCCATAGAA	CCCCACCTCCATCACAA
<i>β-actin</i>	CAAGGTGTCATGGTCGGCAT	GGGTACTTCAGGGTGAGGATAC

(Caldeira and Wicket, 2005; Intergovernmental Panel on Climate Change, 2007; Steinacher et al., 2008). Essential to our ability to forecast how OA will impact marine organisms is an understanding of the mechanisms underlying their physiological capacity to tolerate changes in seawater pH. The transcriptomics approach of the present study has allowed us to capture the changes in gene expression that characterize the initial response to CO₂-driven seawater acidification of developing sea urchin larvae. Following normalization of the microarray data, statistical analysis using empirical Bayes moderated *t*-statistics (Smyth, 2004) revealed subtle but significant changes in the transcriptome of larvae raised in the Moderate CO₂ (pH 7.96±0.01) and High CO₂ (pH 7.88±0.02) conditions when both groups were compared with larvae raised under Control (present) CO₂ conditions (pH 8.01±0.01). Genes were subsequently assigned to broad biological processes in order to determine the larger cellular pathways that were responsive to decreases in seawater pH that characterize OA.

Of the 1057 genes on the microarray, 83 genes had statistically significant fold changes in mRNA transcript levels in response to Moderate CO₂ and gene expression was decreased in response to elevated CO₂ in all cases (Fig. 2A; Table 2). Genes involved in biomineralization, the cellular stress response and energy metabolism accounted for 50% of this global reduction in gene expression (Fig. 2A). Fold changes in expression measured by qPCR

for four biomineralization genes (*cyclophilin*, *MSP130*, *COLP3α*, *P16*) and six genes involved in energy metabolism (*Suclg1*, *Idh3a*, *Sdhb*, *Atp5d*, *Cox5b*, *Ndufs6*) closely matched those measured by microarray analysis (Table 3). Changes in other biological processes were captured in this microarray analysis with translational control, ion regulation and acid–base balance, cell cycle and development accounting for 13.3%, 8.4%, 9.6% and 9.6%, respectively of the significant changes in gene expression.

In response to development under High CO₂, 178 genes had significantly different expression when compared with larvae that developed under Control CO₂ (Fig. 2B; Table 4). Of these 178 genes, 90% (160 genes) had mRNA transcript levels that were significantly decreased in response to High CO₂, with the remaining 10% (18 genes) having elevated expression in response to High CO₂. Genes involved in apoptosis, the cellular stress response, and metabolism accounted for almost 70% of the significantly decreased transcriptomic changes in larvae that developed under High CO₂ (Fig. 2B).

From a physiological perspective these results suggest that in general, larval urchins are not upregulating genes in various pathways to compensate for the effects of acidification and defend cellular homeostasis under elevated CO₂ conditions. Although the transcriptomic responses to Moderate and High CO₂ were distinct, with only 10 shared genes that were differentially regulated in

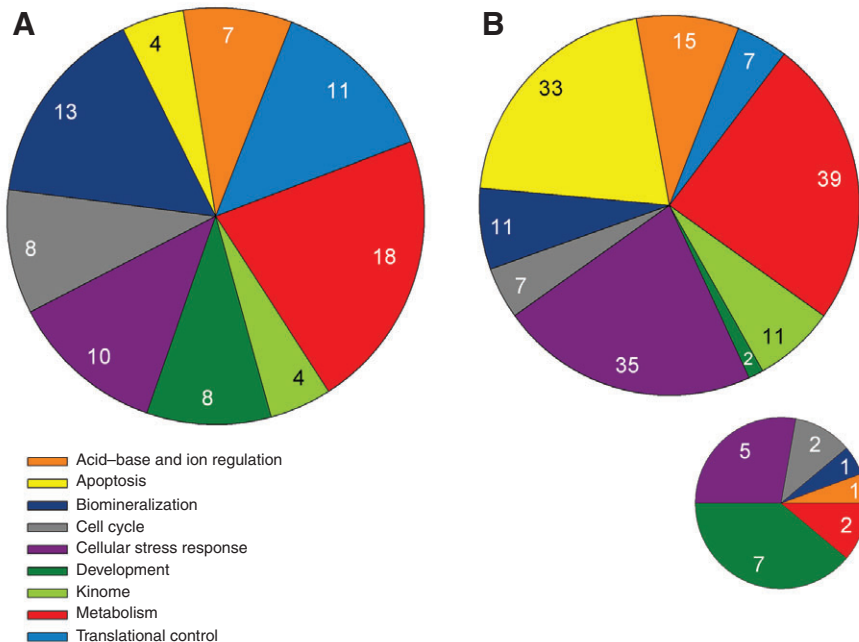


Fig. 2. Representation of genes, grouped by biological process, demonstrating significant fold-changes in mRNA transcript expression between early prism larvae cultured at Moderate CO₂ (A) or High CO₂ (B) and compared to larvae cultured at Control CO₂. Data are presented as the percentage of genes found within a particular group relative to the total number of genes that showed significant changes in expression. Numbers within each piece of the pie chart represent the actual number of genes within a particular biological process. All mRNA transcript levels with significant changes in expression were found to be lower in the Moderate CO₂ group (A) and are presented in a single pie chart. In response to High CO₂ (B), the significant fold changes in gene expression were predominantly found to be decreased in the High CO₂ group (large pie chart) with only 10% of the genes found to be increased in the High CO₂ group (small pie chart). See Tables 2 and 4 for more information on the specific genes in these categories for Moderate CO₂ and High CO₂, respectively.

response to both elevated CO₂ conditions; there was, however, considerable overlap in the biological processes that were regulated

by decreased seawater pH. Overall, the results from this study confirm the importance of some pathways in the physiological

Table 2. Fold changes in gene expression in early prism larvae (40 h post-fertilization) that developed under Moderate CO₂ conditions compared with early prism larvae raised under Control CO₂ conditions

Gene	Gene ID	Fold change (FCUL → FCLL)	Protein information
Acid-base and ion regulation			
<i>Atp13a3</i>	SPU_011933	-2.08 → -1.03	H ⁺ /K ⁺ -ATPase
<i>Aqp</i>	SPU_021388	-1.68 → -1.18	Aquaporin, water and potentially CO ₂ transport
<i>Aqp4</i>	SPU_012222	-1.64 → +1.06	Aquaporin, water transport
<i>Atp7a</i>	SPU_028504	-1.68 → -1.09	Cu ²⁺ -ATPase
<i>Atp1a3</i>	SPU_025815	-1.84 → +1.14	Na ⁺ /K ⁺ -ATPase
<i>Atp6ap1</i>	SPU_012695	-1.60 → +1.05	Vacuolar H ⁺ -ATPase (V-ATPase)
<i>Slc22a13</i>	SPU_027502	-1.58 → -1.01	Organic cation transporter
Apoptosis			
<i>Bruce/BIRC6</i>	SPU_001262	-1.60 → -1.01	Baculoviral IAP repeat-containing 6, inhibitor of apoptosis
<i>Survivin/BIRC5</i>	SPU_008878	-1.63 → +1.07	Baculoviral IAP repeat-containing 5, inhibitor of apoptosis
<i>RAIDD</i>	SPU_023153	-1.56 → +1.01	RIP-associated ICH1/CED3 homologous protein with death domain, Cell Extrinsic apoptosis
<i>Caspase-8-like</i>	SPU_016039	-1.54 → +1.01	Cysteine protease, cell extrinsic apoptosis
Biom mineralization			
<i>cyclophilin 2</i>	SPU_007484	-1.53 → -1.07	Peptidylpropyl <i>cis-trans</i> isomerases
Other cyclophilins	SPU_008305	-1.61 → +1.02	Peptidylpropyl <i>cis-trans</i> isomerases
<i>MSP130</i>	SPU_013821	-1.58 → -1.01	Primary mesenchyme cell (PMC)-specific protein
<i>MSP130-related 3</i>	SPU_013823	-1.65 → -1.01	PMC-specific protein
<i>COLP3α</i>	SPU_003768	-1.53 → -1.02	Most abundant collagen in PMCs, non-fibrillar collagen
<i>COLP4α</i>	SPU_015708	-1.69 → +1.07	Next most abundant collagen, non-fibrillar collagen
Other collagens	SPU_009076	-1.56 → +1.00	Mostly fibrillar collagens
Other collagens	SPU_022116	-1.63 → +1.05	Mostly fibrillar collagens
<i>P19</i>	SPU_004136	-1.65 → +1.05	PMC-specific protein
<i>P16</i>	SPU_018408	-1.55 → -1.06	PMC-specific protein essential for skeletal rod elongation
<i>P16-like</i>	SPU_018405	-1.60 → +1.03	PMC-specific protein essential for skeletal rod elongation
<i>osteonelectin</i>	SPU_028275	-1.61 → 1.00	Glycoprotein that binds calcium
<i>Runt-1</i>	SPU_025612	-1.66 → +1.01	Transcription factor, triggers differentiation of skeletogenic cells
Cell cycle			
<i>Cdc27/Apc3</i>	SPU_022322	-1.59 → +1.04	Anaphase promoting complex 3, ubiquitin-proteolysis pathway
<i>MCM4</i>	SPU_024515	-1.59 → +1.04	Mini chromosome maintenance 4
<i>Psf2</i>	SPU_021616	-1.52 → +1.01	DNA replication complex GINS protein
<i>Chk2</i>	SPU_004975	-1.60 → -1.06	Checkpoint kinase 2
<i>Cyclin T</i>	SPU_021812	-1.58 → -1.01	CDK regulatory subunit involved in transcription
<i>SMC4</i>	SPU_013617	-1.74 → +1.11	Structural maintenance of chromosome 4
<i>CDK8</i>	SPU_001690	-1.56 → +1.02	Cyclin-dependent kinase, initiates transcription
<i>CDK1</i>	SPU_002210	-1.53 → 1.00	Cyclin-dependent kinase, regulates mitosis
Cellular stress response			
Protein homeostasis			
<i>NSFL1C</i>	SPU_015012	-1.66 → -1.04	p97 ATPase cofactor p47, protein degradation
<i>PSMC3</i>	SPU_003847	-1.63 → +1.01	26S proteasome subunit, protein degradation
<i>Hsp40A</i>	SPU_016562	-1.52 → 1.00	40kDa Heat shock protein, co-chaperone of Hsp70
Antioxidant defense			
<i>MGST-3</i>	SPU_016492	-1.84 → -1.01	Glutathione S-transferase, microsomal
<i>GST pi</i>	SPU_017373	-1.66 → +1.08	Glutathione S-transferase, cytosolic
Toxicant, metal and xenobiotic defense			
<i>Cyp3-like16</i>	SPU_014092	-1.74 → -1.03	Cytochrome P450 monooxygenase
<i>Cyp2-like9</i>	SPU_003606	-1.77 → +1.03	Cytochrome P450 monooxygenase
<i>Tf</i>	SPU_026949	-1.65 → +1.03	Homolog of transferrin, metal detoxification
<i>Ugt1-like</i>	SPU_012199	-1.68 → +1.06	UDP glucuronosyltransferase
<i>Shr2</i>	SPU_008117	-1.58 → +1.04	Nuclear receptor that binds estradiol
Development			
<i>Wnt8</i>	SPU_020371	-1.52 → -1.02	Component of gene regulatory network (GRN) that controls differentiation of Skeletogenic micromeres
<i>Blimp1</i>	SPU_027235	-1.68 → -1.05	Stabilizes the GRN thru its interaction with Wnt8
<i>Smad1/5/8</i>	SPU_020722	-1.77 → +1.09	Regulation of transcription, DNA dependent
<i>GataE</i>	SPU_010635	-1.58 → +1.01	GATA-binding transcription factor E, stabilizes GRN
<i>Smad5</i>	SPU_000739	-1.55 → -1.01	Regulation of transcription, DNA dependent
<i>PKS-like</i>	SPU_002895	-1.55 → -1.05	Polyketide synthase, involved in pigmentation
<i>Ap4</i>	SPU_003179	-1.56 → +1.01	Regulation of transcription
<i>Dac</i>	SPU_028061	-1.55 → +1.01	Regulation of transcription, anatomical stru

Table continued on next page.

response to elevated CO₂ (for a review, see Pörtner et al., 2005) as well as provide insight into less targeted cellular pathways that are altered in response to CO₂-driven acidification. In the sections below, we describe the changes in mRNA expression in five main processes (1) acid–base and ion regulation, (2) biomineralization and skeletogenesis, (3) cellular stress response, (4) metabolism and (5) apoptosis.

Acid-base and ion regulation

Much of the physiological research centered on the effects of elevated CO₂ has focused on mechanisms of acid–base regulation since the link between hypercapnia and internal acidosis is well established (for a review, see Heisler, 1989; Portner et al., 2005). Although much of this research was conducted using high levels of environmental CO₂ that are significantly outside the range of predicted atmospheric CO₂ scenarios and resulting OA in the future (Intergovernmental Panel on Climate Change, 2007), they do provide us with a mechanistic framework to begin interpreting our gene expression changes with respect to shifts in acid–base status. The ability to regulate acid–base balance has been investigated in a number of adult urchin species (Spicer, 1995; Burnett et al., 2002;

Miles et al., 2007); however, little is known about the capacity of urchin larvae to compensate for acid–base disturbances. Overall, invertebrates are poor acid–base compensators, especially when compared with vertebrates, and adult urchins specifically are unable to regulate internal acid–base status when exposed to both CO₂-acidified water (1–1.5 pH unit decrease) (Miles et al., 2007) and emersion (Spicer et al., 1988; Burnett et al., 2002).

The primary method of acid–base regulation is ion exchange and a reliance on proton (H⁺) and bicarbonate (HCO₃[−]) transport through Na⁺/H⁺- and Cl[−]/HCO₃[−] exchangers, respectively. As a result, a positive relationship exists between the capacity of a species for ionic regulation and acid–base compensation (Heisler, 1989). Although we did not measure changes in extracellular or intracellular pH that would result from the rapid diffusion of CO₂ and dissociation of carbonic acid into H⁺ and HCO₃[−] ions in different compartments within the animal, the changes in the transcriptome in response to both Moderate and High CO₂ suggest that acid–base compensation and ion regulatory pathways are affected by CO₂-driven seawater acidification (Tables 2 and 4, respectively). There was no significant effect of elevated CO₂ on the mRNA transcript levels of either Na⁺/H⁺- and Cl[−]/HCO₃[−] exchangers suggesting that there was no

Table 2. Continued

Gene	Gene ID	Fold change (FCUL → FCLL)	Protein information
Kinome			
<i>MLCKa</i>	SPU_023876	−1.55 → −1.02	Myosin light chain kinase
<i>MLCKc</i>	SPU_019751	−1.54 → −1.01	Myosin light chain kinase
<i>MAPKAPK5b</i>	SPU_028463	−1.73 → +1.10	Mitogen-activated protein kinase signaling
<i>NLK</i>	SPU_010846	−1.60 → +1.03	Nemo-like kinase
Metabolism – energy metabolism			
Tricarboxylic acid cycle			
<i>Suclg1</i>	SPU_025397	−1.90 → −1.01	Succinyl-CoA synthetase, LG uses GTP
<i>Idh3a</i>	SPU_027710	−1.66 → +1.01	Isocitrate dehydrogenase 3a
<i>Idh3g</i>	SPU_002807	−1.65 → +1.03	Isocitrate dehydrogenase 3g
<i>Sdhb</i>	SPU_026295	−1.70 → +1.09	Succinate dehydrogenase b
<i>Aco2a</i>	SPU_005839	−1.40 → −1.10	Aconitase 2a, mitochondrial
Electron transport chain			
<i>Atp5d</i>	SPU_028873	−1.61 → −1.09	ATP synthase, H ⁺ transporting, F1 complex
<i>Atp5f1</i>	SPU_000022	−1.62 → +1.02	ATP synthase, H ⁺ transporting, F0 complex
<i>Atp5i</i>	SPU_001183	−1.57 → −1.01	ATP synthase, H ⁺ transporting, F0 complex
<i>Ndufs6</i>	SPU_019206	−1.60 → −1.04	NADH dehydrogenase (ubiquinone) Fe-S protein 6
<i>Ndufv2</i>	SPU_026881	−1.66 → +1.08	NADH dehydrogenase (ubiquinone) flavoprotein 2
<i>Ndufa12</i>	SPU_002128	−1.70 → +1.09	NADH dehydrogenase
<i>Uqcrrh</i>	SPU_013225	−1.58 → −1.05	Cytochrome <i>c</i> reductase, hinge protein
<i>Cox4i1</i>	SPU_014478	−1.62 → +1.06	Cytochrome <i>c</i> oxidase
Mitochondrial membrane transporters			
<i>Slc25a5</i>	SPU_004813	−1.86 → −1.18	ADP, ATP carrier protein 2, energy transfer
<i>Slc25a3</i>	SPU_009872	−1.70 → −1.01	Phosphate carrier, energy transfer
Other metabolism genes			
<i>HMGcs1</i>	SPU_007114	−1.53 → −1.03	Hydroxymethylglutaryl-CoA synthase 1, lipid biosynthesis
<i>Acs-like 1</i>	SPU_012875	−1.51 → −1.03	Acyl-CoA synthetase, lipid biosynthesis
<i>Slc23a2</i>	SPU_009217	−1.44 → −1.06	Na ⁺ /L-ascorbic acid transporter, vitamin C transport
Protein synthesis – translational control			
<i>eIF2Bβ</i>	SPU_004173	−1.70 → −1.04	Translation factor – initiation
<i>eIF2γ</i>	SPU_020412	−1.51 → −1.01	Translation factor – initiation
<i>eIF3e</i>	SPU_007226	−1.60 → +1.05	Translation factor – initiation
<i>eIF3j</i>	SPU_013398	−1.80 → −1.08	Translation factor – initiation
<i>eIF3k</i>	SPU_010303	−1.67 → +1.06	Translation factor – initiation
<i>eIF4G</i>	SPU_024859	−1.65 → +1.07	Translation factor – initiation
<i>VARs-B</i>	SPU_002908	−1.55 → −1.02	Translation factor – elongation
<i>VARs-A</i>	SPU_008058	−1.62 → +1.03	Translation factor – elongation
<i>PABPN1</i>	SPU_028828	−1.44 → −1.07	Translation factor – termination
<i>hnRNP K</i>	SPU_008011	−1.64 → +1.02	IRES-dependent translation
<i>PTB</i>	SPU_000961	−1.65 → +1.05	IRES-dependent translation

Data are presented as the upper (FCUL) and lower (FCLL) limits of fold change.

Table 3. Comparison of fold changes in gene expression as measured by DNA microarray analysis and quantitative real-time PCR

Gene	Gene ID	Mean fold change microarray	Mean fold change* qPCR
<i>cyclophilin</i>	SPU_007484	-1.29	-1.21
<i>MSP130</i>	SPU_013821	-1.25	-1.27
<i>COLP3α</i>	SPU_003768	-1.27	-1.27
<i>P16</i>	SPU_018408	-1.28	-1.54
<i>Suclg1</i>	SPU_025397	-1.38	-1.33
<i>ldh3a</i>	SPU_027710	-1.28	-1.11
<i>Sdhb</i>	SPU_026295	-1.25	-1.35
<i>Atp5d</i>	SPU_028873	-1.32	-1.36
<i>Cox5b</i>	SPU_019685	-1.27	-1.21
<i>Ndufs6</i>	SPU_019206	-1.29	-1.25

qPCR, quantitative real-time PCR.

*Relative to the β -actin gene.

direct effect of CO₂-driven acidification on the membrane transport mechanisms important for acid–base compensation at the molecular level. There was, however, decreased expression of a number of important proton (e.g. H⁺/K⁺-ATPase) and other ion transporters, particularly sodium (Na⁺)-dependent ion transporters, suggesting that urchin larvae may be responding to changes in ion gradients that resulted from seawater acidification. Furthermore, exposure to High CO₂ conditions resulted in significantly decreased expression of a number of genes involved in the transport of Na⁺, such as a Na⁺ channel (*Scnn1a*), a Na⁺/Ca²⁺ exchanger (*Slc8a3*), a Na⁺/K⁺/Ca²⁺ exchanger (*Slc24a4*), a Na⁺/K⁺/2Cl⁻ co-transporter (*Slc12a2*) and a number of Na⁺-dependent transporters (e.g. *Slc20a2*, *Slc5a8*). These results suggest that there might be decreased ion transport or transport capacity with increasing CO₂ exposure, and this in turn might affect acid–base regulation, as this process is so tightly linked to solute transport.

In response to both Moderate and High CO₂ conditions, larvae had significantly decreased mRNA levels of a number of different ATPases, which require the hydrolysis of ATP for ion transport. The decrease in ATPases, such as H⁺/K⁺-ATPase and Na⁺/K⁺-ATPase, may represent a potential energy savings strategy in larval urchins since it has been shown that animals shift to more energy efficient transporters, such as Na⁺/H⁺ and Cl⁻/HCO₃⁻ exchangers, during periods of internal acidosis (Pörtner et al., 2000). Finally, in response to High CO₂ conditions, larvae had decreased mRNA levels of a Na⁺/Ca²⁺ exchanger as well as a Na⁺/K⁺/Ca²⁺ exchanger. In combination with the measured decrease in transcripts for a Ca²⁺-ATPase, these data suggest that larvae raised under elevated CO₂ may have a reduced capacity to transport Ca²⁺ to the sites of calcification as a result of disturbances in ion regulation.

It is not possible from the results of the current experiment to determine whether these gene expression changes are in response to elevated internal H⁺ concentrations from the dissociation of H₂CO₃ that has in turn altered the internal ion gradients or are the result of the active suppression of ATP-dependent ion transporters in attempts to minimize energy demand (further discussion in Metabolism section). Future experiments that pair acid–base physiology with gene expression studies will be instrumental in our understanding of the molecular mechanisms regulating acid–base status in response to OA.

Biom mineralization and skeletogenesis

Given the link between CO₂-driven seawater acidification and decreases in carbonate ions in the oceans, research on the organismal

impacts of OA has predominantly centered around calcifying marine organisms, focused largely on calcification (for a review, see Doney et al., 2009). Physiologically, ocean carbonate levels are likely not the drivers of calcification, since generally animals transport bicarbonate across their epithelium from the seawater. However, the effects of internal P_{CO₂} and pH on carbonate speciation within the calcification compartments would follow the same principles, depending on the organism's ability to regulate an internal acidosis and result in the effects on calcification that have been documented in response to elevated CO₂. Although some studies have documented no (Langer et al., 2006) or a positive (Iglesias-Rodriguez et al., 2008; Wood et al., 2008) effect of OA conditions on calcification rate and skeleton formation, the majority of studies have demonstrated that OA conditions negatively impact these processes (e.g. Riebesell et al., 2000; Langdon and Atkinson, 2005; Gazeau et al., 2007; Kurihara et al., 2007; Kuffner et al., 2007). In the present study, mRNA transcripts for genes central to skeletogenesis and the calcification process were decreased in urchins raised under both Moderate CO₂ and High CO₂ conditions (Tables 2 and 4), suggesting that these larvae may not have the capacity to upregulate biomineralization pathways to compensate for the effects of elevated CO₂ under future emission scenarios.

The cellular and molecular mechanisms of biomineralization and skeletogenesis of the echinoderm larval endoskeleton are well documented (for reviews, see Killian and Wilt, 2008; Mann et al., 2008). Skeletogenesis is performed by the primary mesenchyme cells (PMCs), which are responsible for providing the biomineral, amorphous calcium carbonate, and the proteins necessary for the formation of the organic matrix. Although the specific transcripts that changed in expression in response to Moderate CO₂ and High CO₂ conditions differed for the most part, overall there was a consistent downregulation of genes involved in both the sequestration and binding of Ca²⁺ for mineral deposition during spicule formation and skeletogenesis. Culture at Moderate CO₂ and High CO₂ levels resulted in significantly lower mRNA transcript levels of *Msp130*, a gene that encodes a PMC-specific cell surface glycoprotein that is thought to be involved in the binding and sequestration of Ca²⁺ ions to the surface of the PMCs for subsequent deposition into the growing skeleton (Farach-Carson et al., 1989). Similarly, gene expression of the related proteins *Msp130*-related 3 and *Msp130*-related 6 were lower in larvae from Moderate CO₂ and High CO₂ conditions, respectively. Furthermore, mRNA transcripts of a number of genes involved in the binding of Ca²⁺ for skeletogenesis were decreased in response to Moderate CO₂ (e.g. *osteonectin*) and High CO₂ conditions (e.g. *serine rich protein 12*, *SPARC-like* and *Casr*, a Ca²⁺ receptor involved in biomineralization) (Livingston et al., 2006).

Exposure to elevated CO₂ changed the expression patterns of genes in the gene regulatory network (GRN), a series of genes that specify the differentiation of the skeletogenic micromere lineage of cells during larval development in sea urchins (for reviews, see Oliveri et al., 2008; Etensohn, 2009). Key transcription factors, *Wnt8* and *Blimp1* (Table 2, Development), as well as *Runt-1* were significantly decreased in larvae that developed under Moderate CO₂. Similarly, expression of *Alx1* and *Runt-2* (Table 4, Biomineralization) were significantly lower in larvae that developed under High CO₂. Although these particular genes are important during the initiation of this regulatory cascade early in development (<18 h post-fertilization), changes in expression later in development, as measured in the present study (40 h post-fertilization), might still be manifested upstream and affect the activation of genes central to biomineralization in PMCs.

Table 4. Fold changes in gene expression in early prism larvae (40 h post-fertilization) that developed under High CO₂ conditions compared with early prism larvae raised under Control CO₂ conditions

Gene	Gene ID	Fold change (FCUL → FCLL)	Protein information
Acid-base and ion regulation			
<i>Slc8a3</i>	SPU_026183	-1.52 → -1.02	Na ⁺ /Ca ²⁺ exchanger
<i>Slc41a1</i>	SPU_001481	-1.35 → -1.13	mgtE-like Mg ²⁺ transporter
<i>Scnn1a</i>	SPU_014519	-1.43 → -1.07	Sodium channel
<i>Aqp</i>	SPU_023979	-1.40 → -1.09	Aquaporin, water channel
<i>Slc12a2</i>	SPU_004877	-1.35 → -1.12	Na ⁺ /K ⁺ /2Cl ⁻ cotransporter
<i>Slco5a1</i>	SPU_004407	-1.29 → -1.06	Organic anion transporter
<i>Slc39a3</i>	SPU_002226	-1.38 → -1.02	Zinc transporter
<i>Slc24a4</i>	SPU_023689	-1.37 → +1.03	Na ⁺ /K ⁺ /Ca ²⁺ exchanger
<i>Slco</i>	SPU_007603	-1.31 → -1.01	Organic anion transporter
<i>Slc39a8</i>	SPU_023011	-1.33 → +1.02	Zinc transporter
<i>Atp13a4</i>	SPU_005539	-1.26 → -1.03	H ⁺ /K ⁺ -ATPase
<i>Slc20a2</i>	SPU_020699	-1.30 → +1.02	Na-phosphate transporter, type III
<i>Atp2a1</i>	SPU_013051	-1.20 → -1.06	Ca ²⁺ -ATPase
<i>Slc5a8</i>	SPU_012573	-1.30 → -1.06	Na ⁺ -iodide related transporter
<i>Slc5a5</i>	SPU_021781	-1.36 → +1.02	Na ⁺ -iodide symporter
<i>Aqp*</i>	SPU_021388	+1.46 → +1.07	Aquaporin, water channel and potentially CO ₂
Apoptosis			
<i>Caspase 8-like2a</i>	SPU_008540	-1.27 → -1.04	Cysteine protease, cell extrinsic pathway of apoptosis
<i>Caspase 8-like2b</i>	SPU_022177	-1.29 → 1.00	Cysteine protease, cell extrinsic pathway of apoptosis
<i>Caspase 8-like3*</i>	SPU_016039	-1.28 → -1.18	Cysteine protease, cell extrinsic pathway of apoptosis
<i>Caspase 8-like5</i>	SPU_024371	-1.36 → +1.05	Cysteine protease, cell extrinsic pathway of apoptosis
<i>Caspase 3/7-like</i>	SPU_002280	-1.33 → -1.05	Cysteine protease, last caspase in pathway before cell death
<i>caspase N2a</i>	SPU_009497	-1.26 → -1.03	Cysteine protease, N for novel
<i>caspase N2f</i>	SPU_026743	-1.32 → -1.01	Cysteine protease, N for novel
<i>caspase N3a</i>	SPU_017523	-1.46 → +1.02	Cysteine protease, N for novel
<i>caspase N6a</i>	SPU_006866	-1.37 → +1.02	Cysteine protease, N for novel
<i>caspase N6b</i>	SPU_027596	-1.27 → -1.03	Cysteine protease, N for novel
<i>ICE like-1a</i>	SPU_002921	-1.75 → +1.26	Interleukin-converting enzyme, cysteine protease
<i>ICE like-2</i>	SPU_021141	-1.28 → -1.08	Interleukin-converting enzyme, cysteine protease
<i>ICE like-3</i>	SPU_011872	-1.32 → -1.04	Interleukin-converting enzyme, cysteine protease
<i>ICE like-4</i>	SPU_012722	-1.34 → -1.08	Interleukin-converting enzyme, cysteine protease
<i>Tnfsf-like3</i>	SPU_015654	-1.32 → -1.02	Tumor necrosis factor subfamily like 3, ligand for TNFR with death domain
<i>Tnfsf-like1</i>	SPU_009528	-1.38 → +1.04	Tumor necrosis factor subfamily like 1, ligand for TNFR lacking death domain
<i>Tnfrsf1a</i>	SPU_012211	-1.38 → +1.01	Tumor necrosis factor receptor (TNFR) superfamily 1, trigger apoptosis upon binding of Ligand (TNF)
<i>Tnfrsf-like1</i>	SPU_010230	-1.28 → -1.06	TNFR
<i>Tnfrsf-cl1</i>	SPU_010180	-1.36 → 1.00	TNFR, lacks death domain
<i>HVEM/Eda2r-like 1</i>	SPU_024584	-1.37 → +1.01	TNFR, lacks death domain
<i>Troy/Eda2r-like 2</i>	SPU_020740	-1.42 → +1.05	TNFR, lacks death domain
<i>TRAF3</i>	SPU_026495	-1.64 → +1.09	Tnf receptor-associated factor 3, adaptor without death domain
<i>TRAF4</i>	SPU_008332	-1.38 → -1.02	Adaptor without death domain
<i>TRAF6</i>	SPU_028898	-1.47 → +1.08	Adaptor without death domain
<i>BIRC2b</i>	SPU_014057	-1.39 → -1.05	Baculoviral IAP repeat-containing 2, anti-apoptotic
<i>BOK</i>	SPU_021416	-1.33 → -1.05	Bcl2-related ovarian killer, pro-apoptotic
<i>IAP1</i>	SPU_014350	-1.39 → +1.04	Inhibitor of apoptosis 1, anti-apoptotic
<i>Mil2</i>	SPU_001916	-1.40 → +1.05	Bcl-2 protein, pro-apoptotic
<i>Slc22a13</i>	SPU_017736	-1.35 → +1.02	Organic anion transporter, involved in apoptosis
<i>Slc22a15</i>	SPU_019637	-1.24 → -1.05	Organic anion transporter, involved in apoptosis
Biom mineralization			
<i>MSP130*</i>	SPU_013821	-1.42 → -1.05	Primary mesenchyme cell (PMC)-specific protein, cell surface
<i>MSP130-related 6</i>	SPU_014492	-1.31 → -1.02	PMC-specific protein
<i>Runt-2</i>	SPU_007852	-1.34 → -1.09	Transcription factor, triggers differentiation of skeletogenic cells
<i>Alx1</i>	SPU_022817	-1.37 → -1.05	PMC-specific protein, required for skeleton formation
<i>serine rich protein 12</i>	SPU_015338	-1.31 → -1.01	Glycoprotein that binds calcium
<i>SPARC-like</i>	SPU_012548	-1.46 → +1.10	Secreted protein acidic and rich in cysteine, binds Ca ²⁺
<i>Casr</i>	SPU_0017585	-1.26 → -1.04	Calcium receptor
<i>CA-4 likeB</i>	SPU_022346	-1.38 → +1.04	Carbonic anhydrase, catalyzes reversible hydration of CO ₂ to bicarbonate and protons
<i>CA-10 like</i>	SPU_0004135	-1.31 → 1.00	Carbonic anhydrase
<i>CA-8 likeB</i>	SPU_026483	-1.23 → -1.06	Carbonic anhydrase
<i>CA-12 likeB</i>	SPU_025722	-1.21 → -1.06	Carbonic anhydrase
<i>CA-7 likeA</i>	SPU_012518	+1.55 → +1.03	Carbonic anhydrase, extracellular

Table continued on next page.

Table 4. Continued

Gene	Gene ID	Fold change (FCUL → FCLL)	Protein information
Cell cycle			
<i>Cdc23/Apc8</i>	SPU_012696	-1.72 → -1.24	Cell division cycle 23, ubiquitin-proteolysis pathway
<i>Slc29a4</i>	SPU_008397	-1.47 → -1.10	Nucleoside transporter
<i>Slc28a2</i>	SPU_025779	-1.38 → -1.01	Na ⁺ -coupled nucleoside transporter
<i>Apc11</i>	SPU_021695	-1.28 → -1.07	Anaphase promoting complex 11, ubiquitin-proteolysis pathway
<i>Myt1</i>	SPU_008280	-1.32 → -1.04	Tyrosine kinase, inhibits cyclin dependent kinase 1
<i>PFAIRE</i>	SPU_003654	-1.46 → +1.07	Cyclin dependent kinase
<i>Neka</i>	SPU_017790	-1.41 → +1.07	NIMA related kinase, mitotic kinase
<i>SMC1</i>	SPU_021629	+1.46 → +1.05	Structural maintenance of chromosome 1, condensin/cohesin complexes
<i>SMC4*</i>	SPU_013617	+1.31 → 1.00	Structural maintenance of chromosome 4, condensin/cohesin complexes
Cellular stress defense			
Protein homeostasis			
<i>Hsp100B</i>	SPU_006012	-1.44 → +1.04	100kDa heat shock protein, molecular chaperone
<i>Hsp701B</i>	SPU_005808	-1.36 → +1.01	70kDa heat shock protein, molecular chaperone
<i>Hsp701F</i>	SPU_013289	-1.26 → -1.04	70kDa heat shock protein, molecular chaperone
<i>Hsp703A</i>	SPU_014864	-1.33 → 1.00	70kDa heat shock protein, molecular chaperone
<i>Hsp70-like</i>	SPU_021458	-1.32 → +1.03	70kDa heat shock protein, molecular chaperone
<i>Hsp20.1</i>	SPU_001357	-1.19 → -1.12	20kDa heat shock protein, molecular chaperone
<i>Hsp20.2</i>	SPU_020294	-1.32 → 1.00	20kDa heat shock protein, molecular chaperone
<i>UBXD1</i>	SPU_012427	-1.33 → -1.02	UBX domain containing 1, Ub-proteasome pathway
<i>ubiquitin</i>	SPU_015276	+1.38 → +1.15	Ubiquitin-proteasome pathway, signaling
<i>Hsp40A*</i>	SPU_016562	+1.39 → +1.08	40kDa heat shock protein, co-chaperone of Hsp70
Antioxidant defense			
<i>Maf</i>	SPU_025888	-1.36 → -1.07	Transcription factor, oxidative stress-responsive
<i>MGST-2</i>	SPU_008286	-1.48 → +1.08	Glutathione S-transferase, microsomal
<i>GST-12</i>	SPU_023664	-1.32 → 1.00	Glutathione S-transferase, cytosolic
<i>Gpx1</i>	SPU_004397	-1.42 → +1.05	Glutathione peroxidase 7
Toxicant, metal and xenobiotic defense			
<i>Akr1a-like</i>	SPU_027986	-1.31 → -1.10	Aldo-keto reductase
<i>Akr1b-like2</i>	SPU_016996	-1.33 → -1.10	Aldo-keto reductase
<i>Akr1b-like3</i>	SPU_018466	-1.54 → +1.14	Aldo-keto reductase
<i>Cyp2-like9*</i>	SPU_003606	-1.36 → -1.07	Cytochrome P450 monooxygenase, iron homeostasis
<i>Cyp3-like8</i>	SPU_016056	-1.38 → -1.01	Cytochrome P450 monooxygenase
<i>Cyp4-like5</i>	SPU_007558	-1.37 → +1.02	Cytochrome P450 monooxygenase
<i>Cyp2-like14</i>	SPU_006574	-1.21 → -1.08	Cytochrome P450 monooxygenase
<i>Fmo5</i>	SPU_022596	-1.26 → -1.08	Flavin-containing monooxygenase 5
<i>Fmo3</i>	SPU_022597	-1.35 → +1.02	Flavin-containing monooxygenase 3
<i>ABCC9i</i>	SPU_018527	-1.39 → -1.02	ATP-binding cassette superfamily, efflux transporter
<i>ABCG2</i>	SPU_024785	-1.37 → 1.00	ATP-binding cassette superfamily, efflux transporter
<i>Aldh3a1</i>	SPU_009853	-1.32 → 1.00	Aldehyde dehydrogenase
<i>Nat-like</i>	SPU_012976	-1.20 → -1.09	N-acyltransferase-like
<i>NR1H6a</i>	SPU_017404	-1.31 → -1.09	Nuclear receptor subfamily 1 H member 6a
<i>Ark1b-like4</i>	SPU_028344	+1.46 → +1.05	Aldo-keto reductase
<i>Fth1</i>	SPU_004876	+1.52 → +1.07	Heavy chain of ferritin, iron storage
<i>Fmo2</i>	SPU_014947	+1.21 → +1.09	Flavin-containing monooxygenase 2
Adrenergic stress response			
<i>nAChR α7</i>	SPU_013095	-1.37 → -1.01	Acetylcholine receptor, nicotinic
<i>nAChR α9</i>	SPU_005670	-1.36 → +1.00	Acetylcholine receptor, nicotinic
<i>nAChR α4</i>	SPU_019711	-1.56 → +1.17	Acetylcholine receptor, nicotinic
<i>mAChR M5</i>	SPU_016177	-1.45 → +1.07	Acetylcholine receptor, muscarinic
<i>mAChR M4</i>	SPU_019228	-1.30 → -1.02	Acetylcholine receptor, muscarinic
<i>Slc22a3</i>	SPU_006524	-1.39 → -1.04	Monoamine transporter, extraneuronal
<i>Slc6a2</i>	SPU_022506	-1.35 → +1.05	Sodium-dependent noradrenaline transporter
<i>calcineurin</i>	SPU_018404	-1.25 → -1.08	Activates transcription of interleukin 2
<i>SNAP-25</i>	SPU_006859	-1.27 → -1.02	Synaptosome-associated protein
Development			
<i>FoxB</i>	SPU_004551	-1.20 → -1.10	Forkhead box B, transcription factor
<i>Trh</i>	SPU_014249	-1.29 → 1.00	Neuronal PAS domain protein
<i>early-histone-H2a</i>	SPU_002577	+1.62 → +1.03	Involved in nucleosome assembly
<i>FoxQ2</i>	SPU_019002	+1.43 → +1.30	Forkhead box Q2, involved in axis specification
<i>Not</i>	SPU_002129	+1.42 → +1.03	Transcription factor involved in differentiation
<i>PKS-like*</i>	SPU_002895	+1.41 → +1.05	Polyketide synthase, pigment synthesis
<i>Eve</i>	SPU_012253	+1.39 → +1.08	Even-skipped, body morphogenesis
<i>Hes</i>	SPU_021608	+1.28 → +1.14	Hairy/enhancer of split, role in skeletogenic GRN
<i>Otx</i>	SPU_010424	+1.40 → -1.04	Orthodenticle homeobox, role in endomesoderm GRN

Table continued on next page.

Table 4. Continued

Gene	Gene ID	Fold change (FCUL → FCLL)	Protein information
Kinome			
<i>FAK</i>	SPU_019686	-1.30 → -1.11	Focal adhesion kinase, cytoskeletal kinase
<i>KIS</i>	SPU_027616	-1.32 → -1.09	Kinase interacting stathmin, cytoskeletal kinase
<i>MLCKb</i>	SPU_000442	-1.37 → -1.04	Myosin light chain kinase, cytoskeletal kinase
<i>projectin</i>	SPU_013917	-1.33 → -1.06	Cytoskeletal kinase
<i>MAPKAPK5a</i>	SPU_013910	-1.24 → -1.14	Mitogen-activated protein kinase signaling
<i>JAK2</i>	SPU_020082	-1.47 → +1.06	Janus kinase 2, receptor signaling
<i>JAK1</i>	SPU_022495	-1.34 → -1.02	Janus kinase 1, receptor signaling
<i>titin</i>	SPU_005613	-1.23 → -1.11	Cytoskeletal kinase
<i>RIPK1-4A</i>	SPU_005215	-1.27 → -1.06	Receptor-interacting protein kinase, death kinase
<i>LIMK</i>	SPU_022207	-1.56 → +1.17	LIM domain kinase, cytoskeletal kinase
<i>ULK3</i>	SPU_017980	-1.26 → -1.05	Unc-51-like kinase 3, cytoskeletal kinase
Metabolism			
Energy metabolism			
<i>Slc25a5*</i>	SPU_004813	-1.92 → -1.17	ADP, ATP carrier protein 2, energy transfer
<i>Slc25a21</i>	SPU_006682	-1.41 → +1.06	Mitochondrial oxodicarboxylate carrier, energy transfer
<i>Atp5b</i>	SPU_005296	+1.51 → -1.01	ATP synthase, H ⁺ transporting, F1 complex
Carbohydrate metabolism			
<i>glycosidase</i>	SPU_010831	-1.38 → -1.08	Glycosidase, degrades complex carbohydrates
<i>β-D-xylosidase</i>	SPU_021638	-1.34 → 1.00	β-D-xylosidase, glycosidase
<i>Ldh-d</i>	SPU_026206	-1.24 → -1.08	Lactate dehydrogenase d, anaerobic glycolysis
<i>Mdh-1</i>	SPU_023277	-1.33 → +1.05	Malate dehydrogenase 1, citric acid cycle
<i>Pgm</i>	SPU_024573	-1.29 → -1.01	Phosphoglycerate mutase, glycolysis
<i>Pgm2-like1</i>	SPU_028876	-1.51 → +1.13	Phosphoglycerate mutase 2-like 1, glycolysis
<i>Slc5a9</i>	SPU_021455	-1.31 → -1.11	Na ⁺ /glucose cotransporter
<i>Slc5a2</i>	SPU_003667	-1.35 → +1.03	Na ⁺ /glucose transporter, low affinity
<i>Slc5a12</i>	SPU_018791	-1.39 → +1.07	Na ⁺ /glucose cotransporter
<i>Slc2a5</i>	SPU_027868	-1.31 → 1.00	Glucose/fructose transporter
<i>Slc2a13</i>	SPU_017752	-1.30 → +1.01	H ⁺ myo-inositol symporter, glucose transport
<i>Slc37a3</i>	SPU_011768	-1.37 → +1.02	Glycerol-3-phosphate transporter
<i>Slc16a12</i>	SPU_004404	-1.33 → -1.08	Monocarboxylate transporter
<i>Slc16a6</i>	SPU_016408	-1.77 → +1.33	Monocarboxylate transporter
<i>Slc16a4</i>	SPU_009336	-1.53 → +1.17	Monocarboxylate transporter
<i>Slc35a4</i>	SPU_019603	-1.30 → 1.00	UDP-galactose transporter
Amino acid metabolism			
<i>amidase-like</i>	SPU_005666	-1.32 → -1.03	Amidase, hydrolase acting on C–N bonds
<i>amidase-like</i>	SPU_002810	-1.59 → +1.18	Amidase, hydrolase acting on C–N bonds
<i>amidase-like</i>	SPU_017354	-1.29 → -1.03	Amidase, hydrolase acting on C–N bonds
<i>auifite reductase</i>	SPU_019708	-1.55 → +1.14	Sulfite reductase, selenoamino acid metabolism
<i>Slc7a9</i>	SPU_021169	-1.45 → -1.18	Cationic amino acid transporter
<i>Slc7a1</i>	SPU_028697	-1.24 → -1.12	Cationic amino acid transporter
<i>Slc7a6</i>	SPU_004504	-1.25 → -1.09	Cationic amino acid transporter
<i>Slc7a5</i>	SPU_016082	-1.47 → + 1.08	Cationic amino acid transporter, L-type
<i>Slc43a3</i>	SPU_002402	-1.33 → -1.06	FOAP-13, Na ⁺ -independent amino acid transporter
<i>Slc36a1</i>	SPU_022045	-1.43 → +1.06	Proton-coupled amino acid transporter
<i>Slc15a2</i>	SPU_012690	-1.25 → -1.08	H ⁺ /peptide transporter
<i>Slc15a4</i>	SPU_028146	-1.51 → +1.09	Peptide/histidine transporter
<i>Slc7a11</i>	SPU_007905	-1.41 → +1.05	Cystine/glutamate transporter
<i>Slc32a1</i>	SPU_025947	-1.35 → -1.01	GABA and glycine transporter
<i>Dur3</i>	SPU_011497	-1.49 → +1.08	Urea transporter
<i>Slc3a1</i>	SPU_013735	+1.30 → +1.04	Dibasic and neutral amino acid transport
Lipid metabolism			
<i>Accs1</i>	SPU_018270	-1.38 → +1.03	Acyl-CoA synthetase, lipid biosynthesis
<i>Slc5a7</i>	SPU_020026	-1.36 → 1.00	Choline transporter, high affinity
<i>Slc10a2</i>	SPU_023059	-1.29 → -1.04	Na ⁺ bile salt transporter
<i>Slc10a1</i>	SPU_003103	-1.38 → +1.06	Na ⁺ bile salt transporter
Vitamin metabolism			
<i>Slc5a6</i>	SPU_023702	-1.36 → -1.01	Na ⁺ -dependent vitamin transporter
Nucleotide metabolism			
<i>PRPS</i>	SPU_009841	-1.20 → -1.08	Phosphoribosyl pyrophosphate synthetase
Protein synthesis – translational control			
<i>eIF3*</i>	SPU_013398	-1.48 → -1.32	Translation factor – initiation
<i>eIF2Bβ*</i>	SPU_004173	-1.40 → -1.20	Translation factor – initiation
<i>eIF5Bε</i>	SPU_015443	-1.28 → -1.04	Translation factor – initiation
<i>eIF4E-BP</i>	SPU_005957	-1.63 → +1.17	Translation factor – initiation
<i>eIF5B</i>	SPU_001393	-1.67 → 1.06	Translation factor – initiation
<i>eIF2Bα</i>	SPU_024859	-1.65 → 1.07	Translation factor – initiation
<i>UPF3</i>	SPU_000502	-1.32 → -1.07	Up-frameshift protein, translation factor – termination

Data are presented as the upper (FCUL) and lower (FCLL) limits of fold change.

*Genes that were also within the group of mRNA transcripts that changed significantly in response to Moderate CO₂ conditions.

There were a number of differences in the patterns of gene expression in response to the different levels of elevated CO₂ suggesting the degree of CO₂-driven seawater acidification could regulate the biomineralization and skeletogenesis pathway through different mechanisms. Whether these differences will result in differences in growth and structure of the larval skeleton is unknown, but these data provide some of the first information on how this biological process is regulated by extrinsic environmental factors. Larvae that developed under Moderate CO₂ had significantly lower levels of mRNA transcripts for four different collagens as well as for genes that play an important role in skeleton elongation and growth (*P16*, *P16-like* and a number of *cyclophilin* genes; Table 2). Collagens, which are secreted by the PMCs, are essential for the extracellular environment needed by the PMCs as they provide an important substrate for skeletogenesis (Benson et al., 1990). P16 is a small transmembrane protein that is thought to play an important role in skeletal rod elongation (Cheers and Etensohn, 2005). Cyclophilins are a subfamily of the peptidyl prolyl *cis-trans* isomerases and although their exact function is still unknown, their involvement in larval spicule formation is clear (Amore and Davidson, 2007). Larvae that developed under High CO₂ had significantly different levels of five mRNA transcripts that encode for carbonic anhydrase (CA; Table 4). CA catalyzes the hydration of CO₂ and with respect to biomineralization in urchins, this is important for providing the carbonate needed for the mineralization of calcite. It has been shown that inhibitors of CA block spicule formation *in vivo* in developing sea urchins (Mitsunga et al., 1986). There have been 19 CA genes that have been identified in the genome of *S. purpuratus*, but there is little information on the localization and expression patterns of these genes in either the larvae or the adults. Only *CA-7 like A* (*SPU_012518*) has been characterized in urchins and mRNA transcript levels for this gene are highly expressed during skeletogenesis in prism stage larvae and highly expressed in the spines of adult urchins (Livingston et al., 2006). In response to exposure to High CO₂, mRNA transcript levels of *CA-7 like A* were significantly elevated. This was the only gene involved in biomineralization and skeletogenesis found to have significantly increased expression in response to elevated CO₂. The other four CA transcripts with differential expression were all found in significantly lower levels in larvae that were raised under High CO₂ conditions. The involvement of these four CAs in biomineralization has yet to be characterized but given the role of CA in acid-base compensation, it is probable that one or more of them may be regulated by the acid-base imbalance that could have resulted from the decrease in environmental pH.

Cellular stress response

The cellular stress response, also referred to as the defense, is a well-conserved and generalized defense reaction that protects macromolecules (e.g. proteins and DNA) from physical, chemical and biological stressors (for a review, see Kultz, 2005). Although, in animals, early developmental stages are often considered the most vulnerable to changes in environmental conditions, these larval stages have a number of cellular defenses to buffer the effects of environmental stressors (Goldstone et al., 2006; Hamdoun and Epel, 2007). Urchin larvae that developed under both Moderate CO₂ and High CO₂ conditions expressed significantly lower mRNA transcript levels (when compared with Control CO₂ larvae) of a number of genes involved in the cellular stress response, particularly those important for maintaining protein integrity (e.g. molecular chaperones and components of the ubiquitin-proteasome pathway of protein degradation), defending against oxidative stress (e.g.

antioxidants and oxidoreductases) and the efflux and defense against toxicants, metals and xenobiotics (Tables 2 and 4). In addition, development under High CO₂ conditions resulted in urchin larvae having significantly lower expression of a number of mRNA transcripts that are involved in the adrenergic stress, or 'fight or flight', response (Table 4).

As CO₂-driven seawater acidification was increased from Moderate CO₂ to High CO₂ conditions, there was an increase in the number of genes involved in the cellular stress response for which the mRNA transcript levels were significantly downregulated (i.e. from 11 to 35 mRNAs), suggesting a dose-dependent effect of seawater acidification on the cellular stress response. For the most part, these mRNA transcripts were spread between similar cellular defense pathways suggesting that both groups of larvae raised in elevated CO₂ conditions may have reduced capacity to defend the cell against protein denaturing stressors, oxidative damage and chemical and metal toxicity. Larvae raised under Moderate CO₂ and High CO₂ had significantly lower mRNA transcript levels of a number of different heat shock proteins (Hsps) such as Hsp40 under Moderate CO₂ (Table 2) and two Hsp20s, four Hsp70s and Hsp100 under High CO₂ (Table 4). Acting as molecular chaperones, these proteins play an important role in protein quality control and defend the cell from the cytotoxic accumulation of damaged or misfolded proteins (Wickner et al., 1999; Sherman and Goldberg, 2001). Paired with decreases in mRNA transcripts for proteins involved in other aspects of protein homeostasis such as protein folding (*UBXD1*, High CO₂) and degradation (e.g. *PSMC3*, *NSFLIC*, Moderate CO₂), these transcriptomic responses to seawater acidification suggest that these larvae may be unable to defend against protein denaturing stressors.

Exposure to CO₂-driven seawater acidification also resulted in urchin larvae having decreased levels of a number of mRNA transcripts of genes involved in protecting the cell from oxidative damage that results from the generation of reactive oxygen species in response to a variety of stressors, including elevated temperature and toxicants (Lesser, 2006). Specifically, a number of mRNA transcripts for glutathione *S*-transferases were decreased in both the Moderate CO₂ (*MGST-3*, *GST pi*) and the High CO₂ (*MGST-2*, *GST-12*) larvae and for a glutathione peroxidase (*Gpx1*) in the High CO₂ larvae.

Finally, larvae that developed under elevated levels of CO₂ had significantly lower levels of a variety of mRNA transcripts for proteins that are part of the chemical defense against toxicants, metals and xenobiotics (Goldstone et al., 2006). Both groups of larvae that developed under conditions of increased seawater acidification had decreased levels of mRNA transcripts for proteins involved in the oxidative (e.g. cytochrome P450s and flavin-containing monooxygenases) and conjugative (e.g. UDP-glucuronosyl transferases and *N*-acetyl transferases) biotransformation of toxicants and for proteins involved in metal detoxification (e.g. transferrin and ferritin). In addition, larvae that were raised under High CO₂ had significantly lower levels of a number of the ATP-binding cassette (ABC) family of efflux transporters that play an important role in pumping large organic molecules such as toxic compounds out of cells (Hamdoun and Epel, 2007).

The decreased expression of genes that are important in protecting the integrity of the cell in the face of environmental change under modest seawater acidification events (0.05 and 0.13 pH units for Moderate CO₂ and High CO₂, respectively) is somewhat unexpected. These results suggest that either moderate acidification of the seawater had little effect on the integrity of the cell and as a result these pathways were downregulated, or that these larvae did not

have the capacity to maintain these protective mechanisms in the face of elevated CO₂, and that the cellular stress response pathway was impaired at the molecular level. Both scenarios are potentially worrisome and may highlight one of the possible 'costs' for urchin larvae growing up in a high CO₂ world. If the elevated CO₂ exposure results in the downregulation of the cellular stress response, as the gene expression profiles of this study suggest, this could greatly reduce the organism's capacity to tolerate additional stressors, which require similar defense mechanisms. A recent study demonstrated that *S. franciscanus* larvae raised under similar elevated CO₂ conditions as the current study had a reduced and delayed *hsp70* response to heat shock (O'Donnell et al., 2009), lending support to the idea that the cellular stress response may be impaired by exposure to CO₂, at least at the molecular level. Climate change scenarios predict 2–4°C increases in sea surface temperature (Intergovernmental Panel on Climate Change, 2007) and combined with the increased occurrence of hypoxic zones (Chan et al., 2008) in the California Current Large Marine Ecosystem, these subtle changes in gene expression in response to elevated CO₂ may not be trivial in a multi-stressor environment.

Metabolism

The cellular, biochemical and physiological responses of organisms to changes in environmental conditions are very energy demanding processes. As a result, changes in metabolism, routinely measured as changes in metabolic rate, are very common when an organism encounters a novel environment. To minimize energy debt, organisms tend to maintain energy balance, matching energy supply to energy demand (Hochachka and Somero, 2002). How an organism alters its metabolism can tell us a great deal about how an organism is responding to environmental change. An increase in ATP production suggests that there is an increased demand for ATP associated with maintaining cellular homeostasis in the face of changing conditions; whereas a decrease in metabolism can suggest that there is an decreased demand for ATP or that an organism has actively suppressed its metabolism and is waiting for more favorable conditions to return. Exposure of urchin larvae to both Moderate CO₂ and High CO₂ conditions resulted in a significant decrease in mRNA transcripts for a large number of metabolic genes. These transcriptomic changes suggest that metabolism is downregulated in response to CO₂-driven seawater acidification in urchin larvae.

We documented a subtle but unanimous and significant decrease in mRNA levels of genes central to energy metabolism, or the production of ATP, in urchins that developed under Moderate CO₂ (Table 2). This transcriptomic response was evident for genes involved in both the tricarboxylic acid cycle (e.g. succinyl-CoA synthetase and succinate dehydrogenase) and the electron transport chain (e.g. a number of ATP synthases and NADH dehydrogenases). These gene expression profiles suggest that these larvae may either have a reduced demand for ATP and have downregulated this pathway in compensation or that they may have a reduced capacity to generate ATP. It is noteworthy that along with the decreased expression of genes involved in ATP supply through oxidative phosphorylation, culture in Moderate CO₂ conditions resulted in a significant decrease in expression of genes involved in a number of energetically costly processes such as ion regulation using ATPases (e.g. Na⁺/K⁺-ATPase, H⁺/K⁺ ATPase and a V-ATPase) and protein synthesis (e.g. eleven initiation, elongation and termination factors involved in translational control of protein synthesis; Table 2). Protein synthesis and the sodium pump (Na⁺/K⁺-ATPase) are the two biochemical processes with the greatest metabolic demand on developing sea urchin larvae (Leong and

Manahan, 1997; Pace and Manahan, 2006). With the present analysis, it is not possible to determine which came first in the coordinated downregulation of these ATP supply and demand pathways. One explanation is that there is a decrease in ion transport or transport capacity associated with the acid–base disturbance associated with elevated CO₂ (discussed above under Acid–base and ion regulation) and this has decreased the demand for ATP. An alternate explanation is that the decreased expression of genes central to pathways of both energy supply and demand is an indication that these larvae undergoing many of the molecular hallmarks of metabolic suppression.

Metabolic suppression as an adaptive strategy to survive harsh environmental conditions is well documented (Hand, 1991; Guppy and Withers, 1999; Storey and Storey, 2004). Although a number of studies have documented a decrease in metabolic rate (Reipschläger and Pörtner, 1996; Pörtner et al., 1998; Michaelidis et al., 2005; Rosa and Seibel, 2008) and growth (Harris et al., 1999; Michaelidis et al., 2005) with exposure to high CO₂ environments, for the most part these studies have examined the effect of CO₂ levels that are extremely high (~5,000–10,000 p.p.m.) and well above the projected climate change scenarios for the next century. The data here show that urchin larvae could be inducing such a response to a moderate acidification event (0.05 pH unit decrease), something that is considered inevitable in the next 90 years. Suppressing metabolism, through the coordinated downregulation of ATP-utilizing and ATP-generating cellular functions, can prolong an organism's tolerance to a particular environment and therefore can be beneficial in the short-term. However, with chronic metabolic suppression in response to increased CO₂, the costs to the development of urchin larvae could outweigh the short-term benefits and would certainly lead to decreased growth and potential disruption of development in the long-term. Furthermore, the acid–base and ionoregulatory disturbances associated with metabolic suppression (such as decreases in Na⁺/K⁺-ATPase and H⁺/K⁺-ATPase gene expression) could further the 'cost' of this strategy in an environment where these cellular mechanisms are key components of organismal tolerance of elevated CO₂.

Transcriptomic changes of metabolic genes accounted for almost one quarter (24.4%) of all significant changes in gene expression in response to High CO₂. In contrast to the mRNA transcript response to Moderate CO₂ that centered on that pathway of energy metabolism, development under High CO₂ resulted in decreased expression of mRNA transcripts involved in metabolite transport and enzymatic conversion of these metabolites (Goel and Mushegian, 2006). In larvae that developed under High CO₂ conditions, there was a widespread decrease in the mRNA transcripts of genes important to carbohydrate, amino acid and lipid metabolism (Table 4). Although the majority of these decreases in mRNA transcript levels were for genes that encoded metabolic transporters (e.g. glucose transporters involved in carbohydrate metabolism), there was also decreased expression of genes for enzymes that catalyze these metabolites, making them available for energy production (e.g. lactate dehydrogenase and malate dehydrogenase). The transcriptomic response of High CO₂ larvae suggest that these early life history stages may have either a reduced demand or a reduced capacity to mobilize, transport and metabolize sources of fuel necessary to generate the ATP for life's critical functions such as growth or locomotion. Similar to the transcriptomic response to Moderate CO₂, levels of mRNA transcripts for proteins involved in the cellular processes that require ATP, such as ATPases (e.g. H⁺/K⁺-ATPase and Ca²⁺-ATPase) and protein synthesis (e.g. seven translational control factors) were decreased in response to High CO₂. These

changes in the transcriptome may indicate that larvae in High CO₂ conditions are also actively decreasing their demand for ATP.

Taken together, this transcriptomic analysis of metabolic genes in response to two different levels of CO₂-driven seawater acidification suggests that metabolism may be impacted by ocean acidification. Although the underlying mechanisms that regulate metabolism in response to decreased seawater pH appear to be different under the two CO₂ treatments of the current experiment, ultimately they both could influence the capacity of these larvae to metabolize fuel sources and generate ATP. Recent studies in our laboratory have confirmed the effects of a CO₂-driven 0.15 unit decrease in seawater pH (decreased from 7.93 to 7.78) on expression of genes involved in energy metabolism in echinopluteus larvae of another temperate sea urchin, *Lytechinus pictus* (M. J. O'Donnell, A.E.T., M. A. Sewell, L. M. Hammond, K. Ruggiero, N. A. Fangue, M. L. Zippay and G.E.H., submitted). Future studies on both metabolic rate and growth in developing sea urchins are necessary to examine how these changes at the molecular level are transduced at the whole animal level and whether these future ocean conditions will impact organismal performance.

Apoptosis

Apoptosis, or programmed cell death, is an important physiological process for getting rid of unwanted cells (for a review, see Hengartner, 2000). In addition to its role in eliminating cells that have been damaged by stress, disease or mutation, apoptosis plays a critical role in cellular remodeling during development and morphogenesis (Jacobson et al., 1997; Vaux and Korsmeyer, 1999). We documented a wide-spread (33 genes, almost 20% of all significant fold changes in gene expression) decrease in mRNA transcript abundance of numerous genes central to apoptosis in larvae that developed under High CO₂ conditions (Table 4). This is in contrast to the pattern of gene expression that we documented in larvae raised under Moderate CO₂ in which the mRNA transcript levels of only four genes involved in apoptosis were significantly decreased and two of these were negative regulators of apoptosis (e.g. *BIRC5* and *BIRC6*; Table 2). These data could suggest that some threshold was passed with respect to apoptosis under High CO₂ and this pathway was being downregulated in response to seawater acidification.

The process of apoptosis is tightly controlled and can be activated by both intrinsic as well as extrinsic signals through different signaling pathways (Budihardjo et al., 1999). Considerable research has focused on the identification the genes involved in the initiation, execution and regulation of apoptosis in several species (for reviews, see Danial and Korsmeyer, 2004; Riedl and Shi, 2004), including *S. purpuratus* (Robertson et al., 2006). Caspases, a family of cysteine aspartyl proteases, are the executioners of apoptosis (Riedl and Shi, 2004) and different subfamilies of caspases are activated by signals from either the mitochondria (intrinsic pathway) or transmembrane death receptors on the cell surface (extrinsic pathway). Gene expression profiles of the present study suggest that the cell-extrinsic pathway of apoptosis was downregulated by High CO₂. Larvae raised under High CO₂ conditions had decreased mRNA transcript levels of a number of cell surface death receptors (e.g. *Tnfrsf-like1*, *Tnfrsf-cl1*, *HVEM* and *Troy*), some of their specific ligands (e.g. *Tnfrsf-like 1* and *Tnfrsf-like 3*) as well as some of the adaptor molecules (e.g. *TRAF3*, *TRAF4* and *TRAF6*) that transduce the apoptotic signal to the initiator caspases (e.g. *caspase 8-like 2a*, *caspase 8-like 2b* and *caspase 8-like 3*), which were also significantly decreased. The last caspase before cell death, *caspase3/7-like*, which receives signals from both the extrinsic and intrinsic apoptotic signaling pathway,

was also significantly decreased in larvae from the High CO₂ treatment. In addition to the genes with well characterized roles in apoptosis, a number of genes for novel caspases (four genes) as well as ICE-like caspases (five genes) that have only recently been described for sea urchins (Robertson et al., 2006) were found to be expressed in lower levels in larvae raised under High CO₂. Taken together, these gene expression profiles provide insight into the reduced apoptotic capacity of larvae that develop under elevated CO₂ conditions.

Reduced apoptotic capacity could have consequences for development and morphogenesis of new structures and tissues. Although the functionality of apoptosis during development in sea urchins has yet to be demonstrated, apoptosis has been shown to occur in many stages of development (Voronina and Wessel, 2001) as well as during metamorphosis (Roccheri et al., 2002). In this study, we did not see a developmental delay as a consequence of larvae being raised in elevated CO₂ conditions for 40 h (Fig. 1). The results from the current study are consistent with previous research that showed CO₂-driven seawater acidification did not affect early development of sea urchin embryos at pH levels predicted for 2100 by the IPCC [e.g. *Hemicentrotus pulcherrimus* and *Echinometra mathaei* (Kurihara and Shirayama, 2004); *Heliocidaris erythrogramma* (Byrne et al., 2009)]. It is possible that if development was continued under conditions of seawater acidification for longer periods of time that development might be slowed or that developmental abnormalities might increase as a result of the larvae being unable to remodel their cells appropriately during morphogenesis. This may be particularly important in an organism like a sea urchin that has a biphasic life cycle and that undergoes major remodeling during metamorphosis from a bilaterally symmetrical larva to a radially symmetrical juvenile.

Summary and linkages to larval ecology

As demonstrated by significantly lower mRNA transcript levels of genes central to biomineralization, the cellular stress response, metabolism and apoptosis, this study has identified OA scenarios where physiological resistance and tolerance has the potential to fail in larval urchins. Although this is a short duration experiment demonstrating significant but subtle effects at the level of the transcriptome, chronic exposure to elevated CO₂ could culminate in more pronounced physiological changes for larvae during their entire pelagic stage. For example, the inability to compensate for these 'acidified' waters with only 40 h of exposure may have substantial downstream effects on larval development, growth, stress tolerance and settlement. This may be especially critical for urchin larvae in cold-water marine ecosystems. Previous research has shown that changes in ocean temperature could have a profound effect on larval dispersal *via* impacts on planktonic larval duration (O'Connor et al., 2007), with larvae of species found in colder-water habitats spending longer times in the water column. As a result, cold-water species with longer pelagic larval stages would be more vulnerable to OA. Combined with the predictions that high latitude seas are expected to experience the significant impacts of OA very soon (Orr et al., 2005; Steinacher et al., 2008), the ramifications for such a key life-history stage could be significant for the distribution and abundance of cold-temperate purple sea urchins.

As the number of studies on the biological impacts of OA increase, one pattern that is emerging is that there is variation in the response to OA, something that might not be unexpected given the differences in the habitats, life history strategies and evolutionary history of different taxa (Fabry, 2008; Andersson et al., 2008; Aronson et al., 2009). This diversity of biological responses makes

it difficult to make strong predictions about the future impacts of OA and define caps for atmospheric CO₂ emissions to best protect our marine ecosystems. In addition, our inability at present to separate out the effects of pH on acid–base status from that of CO₂ directly, limits our mechanistic understanding of the species-specific sensitivity of various physiological processes to CO₂-driven ocean acidification. A genomics-based approach using transcriptomics to assess physiological capacity in diverse taxa may be an important tool in identifying the common ‘weak links’ in physiological function that prevent an organism from tolerating any additional acidification of their marine environment. It is clear from the present study that pathways other than calcification are impacted greatly, suggesting that overall physiological capacity, and not just a singular focus on biomineralization processes, is essential to our understanding of the costs and consequences of living in a high CO₂ ocean.

The authors would like to thank Dr Bruce Menge, Dr Mary Sewell and Dr Jane Lubchenco for their constructive comments on the manuscript. In addition, we thank Dr Nann Fanguie for help with data collection, Dr Katya Ruggiero for help with microarray normalization and analysis and Scott Simon for assistance with collection of *S. purpuratus* (CA Scientific Collecting Permit #SC-001223). This research was supported by NSF grant OCE-0425107 to G.E.H. This is contribution number 341 from PISCO, the Partnership for Interdisciplinary Studies of Coastal Oceans, funded primarily by the Gordon and Betty Moore Foundation and David and Lucile Packard Foundation.

REFERENCES

- Amore, G. and Davidson, E. H. (2007). *cis*-Regulatory control of cyclophilin, a member of the ETS-DRI skeletogenic gene battery in the sea urchin embryo. *Dev. Biol.* **293**, 555–564.
- Andersson, A. J., Mackenzie, F. T. and Bates, N. R. (2008). Life on the margin: implications of ocean acidification on Mg-calcite, high latitude and cold-water marine calcifiers. *Mar. Ecol. Prog. Ser.* **373**, 265–273.
- Aronson, R. B., Moody, R. M., Ivany, L. C., Blake, D. B., Werner, J. E. and Glass, A. (2009). Climate change and trophic response of the Antarctic bottom fauna. *PLoS One* **4**, e4385.
- Bell, G. and Collins, S. (2008). Adaptation, extinction and global change. *Evol. Appl.* **1**, 3–16.
- Benson, S., Smith, L., Wilt, F. and Shaw, R. (1990). The synthesis and secretion of collagen by cultured sea urchin micromeres. *Exp. Cell Res.* **188**, 141–146.
- Berge, J. A., Bjerkeng, B., Pettersen, O., Schaanning, M. T. and Oxnevad, S. (2006). Effects of increased seawater concentrations of CO₂ on the growth of the bivalve *Mytilus edulis* L. *Chemosphere* **62**, 681–687.
- Buckley, B. A., Gracey, A. Y. and Somero, G. N. (2006). The cellular response to heat stress in the goby *Gillichthys mirabilis*: a cDNA microarray and protein level analysis. *J. Exp. Biol.* **209**, 2660–2677.
- Budihardjo, I., Oliver, H., Lutter, M., Luo, X. and Wang, X. (1999). Biochemical pathways of caspase activation during apoptosis. *Annu. Rev. Cell Dev. Biol.* **15**, 269–290.
- Burnett, L., Terwilliger, N., Carroll, A., Jorgensen, D. and Scholnick, D. (2002). Respiratory and acid-base physiology of the purple sea urchin, *Strongylocentrotus purpuratus*, during air exposure: presence and function of a facultative lung. *Biol. Bull.* **203**, 42–50.
- Byrne, M., Ho, M., Selvakumaraswamy, P., Ngyuen, H. D., Dworjanyn, S. A. and Davis, A. R. (2009). Temperature, but not pH, compromises sea urchin fertilization and early development under near-future climate change scenarios. *Proc. Biol. Sci.* **276**, 1883–1888.
- Caldeira, K. and Wicket, M. E. (2005). Ocean model predictions of chemistry changes from carbon dioxide emissions to the atmosphere and ocean. *J. Geophys. Res.* **110**, C09S04.
- Cameron, J. N. (1986). Acid-base equilibria in invertebrates. In *Acid-Base Regulation in Animals* (ed. N. Heisler), pp. 357–394. New York: Elsevier.
- Chan, F., Barth, J. A., Lubchenco, J., Kirincich, A., Weeks, H., Peterson, W. T. and Menge, B. A. (2008). Emergence of anoxia in the California Current Large Marine Ecosystem. *Science* **319**, 920.
- Cheers, M. S. and Ettensohn, C. A. (2005). P16 is an essential regulator of skeletogenesis in the sea urchin embryo. *Dev. Biol.* **283**, 384–396.
- Chomczynski, P. and Sacchi, N. (1987). Single-step method of RNA isolation by acid guanidinium thiocyanate-phenol-chloroform extraction. *Anal. Biochem.* **162**, 156–159.
- Cohen, A. L. and McConnaughey, T. A. (2003). A geochemical perspective on coral mineralization. In *Biomineralization: Reviews in Mineralogy and Geochemistry* (ed. P. M. Dove, S. Weiner and J. J. DeYoreo), pp. 151–157. Washington, DC: Mineralogy Society of America.
- Cooper, T. F., De'ath, G., Fabricius, K. E. and Lough, J. M. (2008). Declining coral calcification in massive *Porites* in two nearshore regions of the northern Great Barrier Reef. *Glob. Chang. Biol.* **14**, 529–538.
- Daniel, N. N. and Korsmeyer, S. J. (2004). Cell death: critical control points. *Cell* **116**, 205–219.
- De'ath, G., Lough, J. M. and Fabricius, K. E. (2009). Declining coral calcification on the Great Barrier Reef. *Science* **323**, 116–119.
- DeSalvo, M. K., Voolstra, C. R., Sunagawa, S., Schwarz, J. A., Stillman, J. H., Coffroth, M. A., Szmant, M. and Medina, M. (2008). Differential gene expression during thermal stress and bleaching in the Caribbean coral *Montastraea faveolata*. *Mol. Ecol.* **17**, 3952–3971.
- Doney, S. C., Fabry, V. J., Feely, R. A. and Kleypas, J. A. (2009). Ocean acidification: the other CO₂ problem. *Annu. Rev. Mar. Sci.* **1**, 169–192.
- Dupont, S., Havenhand, J., Thorndyke, W., Peck, L. and Thorndyke, M. (2008). Near-future level of CO₂-driven ocean acidification radically affects larval survival and development in the brittlestar *Ophiotrix fragilis*. *Mar. Ecol. Prog. Ser.* **373**, 285–294.
- Ettensohn, C. A. (2009). Lessons from a gene regulatory network: echinoderm skeletogenesis provides insights into evolution, plasticity and morphogenesis. *Development* **136**, 11–21.
- Evans, T. G. and Somero, G. N. (2008). A microarray-based transcriptomic time-course of hyper- and hypo-osmotic stress signaling events in the euryhaline fish *Gillichthys mirabilis*: osmosensors to effectors. *J. Exp. Biol.* **211**, 3636–3649.
- Fabry, V. J. (2008). Marine calcifiers in a high-CO₂ ocean. *Science* **320**, 1020–1022.
- Fabry, V. J., Seibel, B. A., Feely, R. A. and Orr, J. C. (2008). Impacts of ocean acidification on marine fauna and ecosystem processes. *ICES J. Mar. Sci.* **65**, 414–432.
- Farach-Carson, M. C., Carson, D. D., Collier, J. L., Lennarz, W. J., Park, H. R. and Wright, G. C. (1989). A calcium-binding, asparagine-linked oligosaccharide is involved in skeleton formation in the sea urchin embryo. *J. Cell Biol.* **109**, 1289–1299.
- Fu, F. X., Warner, M. E., Zhang, Y., Feng, Y. and Hutchins, D. A. (2007). Effects of increased temperature and CO₂ on photosynthesis, growth, and elemental ratios in marine *Synechococcus* and *Prochlorococcus* (Cyanobacteria). *J. Phycol.* **43**, 485–496.
- Gazeau, F., Quiblier, C., Jansen, J., Gattuso, J. P., Middleburg, J. and Heip, C. (2007). Impact of elevated CO₂ on shellfish calcification. *Geophys. Res. Lett.* **34**, 1–15.
- Goel, M. and Mushegian, A. (2006). Intermediary metabolism in sea urchin: the first inferences from the genome sequence. *Dev. Biol.* **300**, 282–292.
- Goldstone, J. V., Hamdoun, A., Cole, B. J., Howard-Ashby, M., Nebert, D. W., Scally, M., Dean, M., Epel, D., Hahn, M. E. and Stegeman, J. J. (2006). The chemical defensome: environmental sensing and response genes in the *Strongylocentrotus purpuratus* genome. *Dev. Biol.* **300**, 366–384.
- Gracey, A. Y. (2007). Interpreting physiological responses to environmental change through gene expression profiling. *J. Exp. Biol.* **209**, 1584–1592.
- Gracey, A. Y., Troll, J. V. and Somero, G. N. (2001). Hypoxia-induced gene expression profiling in the euryoxic fish *Gillichthys mirabilis*. *Proc. Natl. Acad. Sci. USA* **98**, 1993–1998.
- Gracey, A. Y., Fraser, E. J., Li, W., Fang, Y., Taylor, R. R., Rogers, J., Brass, A. and Cossins, A. R. (2004). Coping with cold: an integrative, multitissue analysis of the transcriptome of a poikilothermic vertebrate. *Proc. Natl. Acad. Sci. USA* **101**, 16970–16975.
- Gracey, A. Y., Chaney, M. L., Boomhower, J. P., Tyburczy, W. R., Connor, K. and Somero, G. N. (2008). Rhythms of gene expression in a fluctuating intertidal environment. *Curr. Biol.* **18**, 1501–1507.
- Guinotte, J. M. and Fabry, V. J. (2008). Ocean acidification and its potential effects on marine ecosystems. *Ann. NY Acad. Sci.* **1134**, 320–342.
- Guppy, M. and Withers, P. (1999). Metabolic depression in animals: physiological perspectives and biochemical generalizations. *Biol. Rev.* **74**, 1–40.
- Hall-Spencer, J. M., Rodolfo-Metalpa, R., Martin, S., Ransome, E., Fine, M., Turner, S. M., Rowley, S. J., Tedesco, D. and Buia, M. C. (2008). Volcanic carbon dioxide vents reveal ecosystem effects of ocean acidification. *Nature* **454**, 96–99.
- Halpern, B. S., Walbridge, S., Selkoe, K. A., Kappel, C. V., Micheli, F., D'Agrosa, C., Bruno, J. F., Casey, K. S., Ebert, C., Fox, H. E. et al. (2008). A global map of human impact on marine ecosystems. *Science* **319**, 948–952.
- Hamdoun, A. and Epel, D. (2007). Embryo stability and vulnerability in an always changing world. *Proc. Natl. Acad. Sci. USA* **104**, 1745–1750.
- Hand, S. C. (1991). Metabolic dormancy in aquatic invertebrates. In *Advances in Comparative and Environmental Physiology*, vol. 8 (ed R. Gilles), pp. 1–50. Heidelberg: Springer Verlag.
- Harris, J. O., Maguire, G. B., Edwards, S. J. and Hindrum, S. M. (1999). Effect of pH on growth rate, oxygen consumption rate, and histopathology of gill and kidney tissue for juvenile greenlip abalone, *Haliotis laevis* Donovan and blacklip abalone, *Haliotis rubra* Leach. *J. Shellfish Res.* **18**, 611–619.
- Hart, M. W. and Strathmann, R. R. (1994). Functional consequences of phenotypic plasticity in echinoid larvae. *Biol. Bull.* **186**, 291–299.
- Hauton, C., Tyrell, T. and Williams, J. (2009). The subtle effects of seawater acidification on the amphipod *Gammarus locusta*. *Biogeosci. Discuss.* **6**, 919–946.
- Heisler, N. (1989). Interaction between gas exchange, metabolism and ion transport in animals. An overview. *Can. J. Zool.* **67**, 2923–2935.
- Hengartner, M. O. (2000). The biochemistry of apoptosis. *Nature* **407**, 770–776.
- Hochachka, P. W. and Somero, G. N. (2002). *Biochemical Adaptation: Mechanism and Process in Physiological Evolution*. New York: Oxford University Press.
- Hoegh-Guldberg, O., Mumby, P. J., Hooten, A. J., Steneck, R. S., Greenfield, P., Gomez, E., Harvell, C. D., Sale, P. F., Edwards, A. J., Caldeira, K. et al. (2007). Coral reefs under rapid climate change and ocean acidification. *Science* **318**, 1737–1742.
- Iglesias-Rodriguez, M. D., Halloran, P. R., Rickaby, R. E. M., Hall, I. R., Colmenero-Hidalgo, E., Gittins, J. R., Green, D. R. H., Tyrrell, T., Gibbs, S. J., von Dassow, P. et al. (2008). Phytoplankton calcification in a high-CO₂ world. *Science* **320**, 336–340.
- Intergovernmental Panel on Climate Change (2007). *Climate Change 2007: The Physical Science Basis. Working Group I Contribution to the Fourth Assessment Report of the Intergovernmental Panel on Climate Change*. Cambridge: Cambridge University Press.

- Jacobson, M. D., Weil, M. and Raff, M. C. (1997). Programmed cell death in animal development. *Cell* **88**, 347-354.
- Killian, C. E. and Wilt, F. H. (2008). Molecular aspects of biomineralization of the echinoderm endoskeleton. *Chem. Rev.* **108**, 4463-4474.
- Kleypas, J. A., Buddemeier, R. W., Archer, D., Gattuso, J. P., Langdon, C. and Opdyke, B. N. (1999). Geochemical consequences of increased atmospheric carbon dioxide on coral reefs. *Science* **284**, 118-120.
- Kuffner, I. B., Andersson, A. J., Jokiel, P. L., Rodgers, K. S. and MacKenzie, F. T. (2007). Decreased abundance of crustose coralline algae due to ocean acidification. *Nature Geosci.* **1**, 114-117.
- Kültz, D. (2005). Molecular and evolutionary basis of the cellular stress response. *Annu. Rev. Physiol.* **67**, 225-257.
- Kurihara, H. (2008). Effects of CO₂-driven ocean acidification on the early developmental stages of invertebrates. *Mar. Ecol. Prog. Ser.* **373**, 275-284.
- Kurihara, H. and Shirayama, Y. (2004). Effects of increased atmospheric CO₂ on sea urchin early development. *Mar. Ecol. Prog. Ser.* **274**, 161-169.
- Kurihara, H., Kato, S. and Ishimatsu, A. (2007). Effects of increased pCO₂ on early development of the oyster *Crassostrea gigas*. *Aquat. Biol. Abstr.* **1**, 91-98.
- Langdon, C. and Atkinson, M. J. (2005). Effect of elevated pCO₂ on photosynthesis and calcification of corals and interactions with seasonal change in temperature/irradiance and nutrient enrichment. *J. Geophys. Res.* **110**, C09S07.
- Langer, C., Geisen, M., Baumann, K. H., Kläs, J., Riebesell, U., Thoms, S. and Young, J. R. (2006). Species-specific responses of calcifying algae to changing seawater carbonate chemistry. *Geochim. Geophys. Geosyst.* **7**, Q09006.
- Leong, P. and Manahan, D. (1997). Metabolic importance of Na⁺/K⁺-ATPase activity during sea urchin development. *J. Exp. Biol.* **200**, 2881-2892.
- Lesser, M. P. (2006). Oxidative stress in marine environments: biochemistry and physiological ecology. *Annu. Rev. Physiol.* **68**, 253-278.
- Livingston, B. T., Killian, C. E., Wilt, F., Cameron, A., Landrum, M. J., Ermolaeva, O., Sapojnikov, V., Maglott, D. R., Buchanan, A. M. and Ettensohn, C. A. (2006). A genome-wide analysis of biomineralization-related proteins in the sea urchin *Strongylocentrotus purpuratus*. *Dev. Biol.* **300**, 335-348.
- Mann, K., Poustka, A. J. and Mann, M. (2008). The sea urchin (*Strongylocentrotus purpuratus*) test and spine proteome. *Proteome Sci.* **6**, 22.
- Manno, C., Sandrini, S., Tositti, L. and Accornero, A. (2007). First stages of degradation of *Limacina helicina* shells observed above the aragonite chemical lysocline in Terra Nova Bay (Antarctica). *J. Mar. Syst.* **68**, 91-102.
- Mayor, D. J., Matthews, C., Cook, K., Zuur, A. F. and Hay, S. (2007). CO₂-induced acidification affects hatching success in *Calanus finmarchicus*. *Mar. Ecol. Prog. Ser.* **350**, 91-97.
- McConnaughey, T. A. and Whelan, J. F. (1997). Calcification generates protons for nutrient and bicarbonate uptake. *Earth Sci. Rev.* **42**, 95-117.
- Michaelidis, B., Ouzounis, C., Palaras, A. and Pörtner, H. O. (2005). Effects of long-term moderate hypercapnia on acid-base balance and growth rate in marine mussels *Mytilus galloprovincialis*. *Mar. Ecol. Prog. Ser.* **293**, 109-118.
- Miles, H., Widdicombe, S., Spicer, J. I. and Hall-Spencer, J. (2007). Effects of anthropogenic seawater acidification on acid-base balance in the sea urchin *Psammechinus miliaris*. *Mar. Pollut. Bull.* **54**, 89-96.
- Mitsunaga, K., Akasaka, K., Shimada, H., Fujino, Y., Yasumasa, I. and Numanoi, H. (1986). Carbonic anhydrase activity in developing sea urchin embryos with special reference to calcification of spicules. *Cell Differ.* **18**, 257-262.
- Nordberg, E. K. (2005). YODA: selecting signature oligonucleotides. *Bioinformatics* **21**, 1365-1370.
- O'Connor, M. I., Bruno, J. F., Gaines, S. D., Halpern, B. S., Lester, S. E., Kinlan, B. P. and Weiss, J. M. (2007). Temperature control of larval dispersal and the implications for marine ecology, evolution, and conservation. *Proc. Natl. Acad. Sci. USA* **104**, 1266-1271.
- O'Donnell, M. J., Hammond, L. M. and Hofmann, G. E. (2009). Predicted impact of ocean acidification on a marine invertebrate: elevated CO₂ alters response to thermal stress in sea urchin larvae. *Mar. Biol.* **156**, 439-446.
- Oliveri, P., Tu, Q. and Davidson, E. H. (2008). Global regulatory logic for specification of an embryonic cell lineage. *Proc. Nat. Acad. Sci. USA* **105**, 5955-5962.
- Olohan, L. A., Li, W., Wulff, T., Jarmer, H., Gracey, A. Y. and Cossins, A. R. (2008). Detection of anoxia-responsive genes in cultured cells of the rainbow trout *Oncorhynchus mykiss* (Walbaum), using an optimized, genome-wide oligoarray. *J. Fish. Biol.* **72**, 2170-2186.
- Orr, J. C., Fabry, V. J., Aumont, O., Bopp, L., Doney, S. C., Feely, R. A., Gnanadesikan, A., Gruber, N., Ishida, A., Joos, F. et al. (2005). Anthropogenic ocean acidification over the twenty-first century and its impact on calcifying organisms. *Nature* **437**, 681-686.
- Pace, D. A. and Manahan, D. T. (2006). Fixed metabolic costs for highly variable rates of protein synthesis in sea urchin embryos and larvae. *J. Exp. Biol.* **209**, 158-170.
- Pearse, J. S. (2006). Ecological role of purple sea urchins. *Science* **314**, 940-941.
- Place, S. P., O'Donnell, M. J. and Hofmann, G. E. (2008). Gene expression in the intertidal mussel *Mytilus californianus*: physiological response to environmental factors on a biogeographical scale. *Mar. Ecol. Prog. Ser.* **356**, 1-14.
- Pörtner, H. O. (2008). Ecosystem effects of ocean acidification in times of ocean warming: a physiologist's view. *Mar. Ecol. Prog. Ser.* **373**, 203-217.
- Pörtner, H. O. and Farrell, A. P. (2008). Physiology and climate change. *Science* **322**, 690-692.
- Pörtner, H. O., Reipschläger, A. and Heisler, R. (1998). Acid-base regulation, metabolism and energetics in *Sipunculus nudus* as a function of ambient carbon dioxide level. *J. Exp. Biol.* **201**, 43-54.
- Pörtner, H. O., Bock, C. and Reipschläger, A. (2000). Modulation of the cost of pH regulation during metabolic depression: a ³¹P-NMR study of the invertebrate (*Sipunculus nudus*) isolated muscle. *J. Exp. Biol.* **203**, 2417-2428.
- Pörtner, H. O., Langenbuch, M. and Michaelidis, B. (2005). Synergistic effects of temperature extremes, hypoxia, and increases in CO₂ on marine animals: from earth history to global change. *J. Geophys. Res.* **110**, C09S10.
- R Development Core Team (2008). *R: A Language and Environment For Statistical Computing*. Vienna: R Foundation for Statistical Computing.
- Reipschläger, A. and Pörtner, H. O. (1996). Metabolic depression during environmental stress: the role of extra- versus intra-cellular pH in the *Sipunculus nudus*. *J. Exp. Biol.* **199**, 1801-1807.
- Riebesell, U., Zondervan, I., Rost, B., Tortell, P. D., Zeebe, R. E. and Morel, F. M. M. (2000). Reduced calcification of marine plankton in response to increased atmospheric CO₂. *Nature* **407**, 364-367.
- Riedl, S. J. and Shi, Y. (2004). Molecular mechanisms of caspase regulation during apoptosis. *Nat. Rev. Mol. Cell Biol.* **5**, 897-907.
- Robertson, A. J., Croce, J., Carbonneau, S., Voronina, E., Miranda, E., McClay, D. R. and Coffman, J. A. (2006). The genomic underpinnings of apoptosis in *Strongylocentrotus purpuratus*. *Dev. Biol.* **300**, 321-334.
- Roccheri, M. C., Tipa, C., Bonaventura, R. and Matranga, V. (2002). Physiological and induced apoptosis in sea urchin larvae undergoing metamorphosis. *Int. J. Dev. Biol.* **46**, 801-806.
- Rosa, R. and Seibel, B. A. (2008). Synergistic effects of climate-related variables suggest future physiological impairment in an oceanic predator. *Proc. Natl. Acad. Sci. USA* **105**, 20776-20780.
- Sabine, C. L., Feely, R. A., Gruber, N., Key, R. M., Lee, K., Bullister, J. L., Wanninkhof, R., Wong, C. S., Wallace, D. W. R., Tilbrook, B. et al. (2004). The oceanic sink for anthropogenic CO₂. *Science* **305**, 367-371.
- Sea Urchin Genome Sequencing Consortium (2006). The genome of the sea urchin *Strongylocentrotus purpuratus*. *Science* **314**, 941-952.
- Seibel, B. A. and Walsh, P. J. (2003). Biological implications of deep-sea carbon dioxide injection inferred from indices of physiological performance. *J. Exp. Biol.* **206**, 641-650.
- Sherman, M. and Goldberg, A. L. (2001). Cellular defenses against unfolded proteins: a cell biologist thinks about neurodegenerative diseases. *Neuron* **29**, 15-32.
- Shirayama, Y. and Thornton, H. (2005). Effect of increased atmospheric CO₂ on shallow water marine benthos. *J. Geophys. Res. Oceans* **110**, C09S08.
- Smyth, G. K. (2004). Linear models and empirical bayes methods for assessing differential expression in microarray experiments. *Stat. Appl. Genet. Mol. Biol.* **3**, Article 3.
- Smyth, G. K. (2005). Limma: linear models for microarray data. In *Bioinformatics and Computational Biology Solutions using R and Bioconductor* (ed. R. Gentleman, V. Carey, S. Dudoit, R. Irizarry and W. Huber), pp. 397-420. New York: Springer-Verlag.
- Spicer, J. I. (1995). Oxygen and acid-base status of the sea urchin *Psammechinus miliaris* during environmental hypoxia. *Mar. Biol.* **124**, 71-76.
- Spicer, J. I., Taylor, A. C. and Hill, A. D. (1988). Acid-base status in the sea urchins *Psammechinus miliaris* and *Echinus esculentus* (Echinodermata: Echinoidea) during emersion. *Mar. Biol.* **99**, 527-534.
- Steinacher, M., Joos, F., Frölicher, T. L., Plattner, G. K. and Doney, S. C. (2008). Imminent ocean acidification projected with the NCAR global coupled carbon cycle-climate model. *Biogeosci. Discuss.* **5**, 4353-4393.
- Storey, K. B. and Storey, J. M. (2004). Metabolic rate depression in animals: transcriptional and translational controls. *Biol. Rev.* **79**, 207-233.
- Strathmann, M. F. (1987). *Reproduction and Development of Marine Invertebrates of the Northern Pacific Coast*. Seattle, WA: University of Washington Press.
- Teranishi, K. S. and Stillman, J. H. (2007). A cDNA microarray analysis of the response to heat stress in hepatopancreas tissue of the porcelain crab *Petrolisthes cinctipes*. *Comp. Biochem. Physiol. D* **2**, 53-62.
- Truchot, J. P. (1987). *Comparative Aspects of Extracellular Acid-Base Balance*. Berlin: Springer-Verlag.
- Vaux, D. L. and Kosmeyer, S. J. (1999). Cell death in development. *Cell* **96**, 245-254.
- Voronina, E. and Wessel, G. M. (2001). Apoptosis in sea urchin oocytes, eggs, and early embryos. *Mol. Reprod. Dev.* **60**, 553-561.
- Watanabe, Y., Yamaguchi, A., Ishida, H., Harimoto, T., Suzuki, S., Sekido, Y., Ikeda, T., Shirayama, Y., Takahashi, M. M., Ohsumi, T. et al. (2006). Lethality of increasing CO₂ levels on deep-sea copepods in the western North Pacific. *J. Oceanogr.* **62**, 185-196.
- Wickner, S., Maurizi, M. R. and Gottesman, S. (1999). Posttranslational quality control: folding, refolding and degrading proteins. *Science* **286**, 1888-1893.
- Widdicombe, S. and Spicer, J. I. (2008). Predicting the impact of ocean acidification on benthic biodiversity: what can animal physiology tell us? *J. Exp. Mar. Biol. Ecol.* **366**, 187-197.
- Wilt, F. H. (2005). Developmental biology meets material science: morphogenesis of biomineralized structures. *Dev. Biol.* **280**, 15-25.
- Wood, H. L., Spicer, J. I. and Widdicombe, S. (2008). Ocean acidification may increase calcification rates, but at a cost. *Proc. Biol. Sci.* **275**, 1767-1773.
- Wootton, J. T., Pfister, C. A. and Forester, J. D. (2008). Dynamic patterns and ecological impacts of declining ocean pH in a high-resolution multi-year dataset. *Proc. Nat. Acad. Sci. USA* **105**, 18848-18853.
- Yang, Y. H., Dudoit, S., Luu, P., Lin, D. M., Peng, V., Ngai, J. and Speed, T. P. (2002). Normalization for cDNA microarray data: a robust composite method addressing single and multiple slide systematic variation. *Nucleic Acids Res.* **30**, e15.